Applications of QCD Sum Rules at Finite Temperature

Yingwen Zhang

Supervisor: Emeritus Professor C.A. Dominguez
Co-Supervisor: Professor A. Peshier

Department of Physics, University of Cape Town

Submitted 11 January 2013
Revised 26 April 2013

Declaration

I declare that this dissertation is my own, unaided work. It is being submitted for the degree of Doctor of Philosophy in Theoretical Physics in the University of Cape Town. It has not been submitted before for any degree or examination in any other university.

Signature of Author ..... Signed by candidate .....

Cape Town
December 2012

Abstract

QCD Sum Rules is one of the most successful quantum field theory frameworks to extract hadronic information from QCD analytically. This technique is based on the Operator Product Expansion (OPE) and Cauchy's Theorem in the complex energy plane. OPE factorizes the short and long distance interactions where the former are calculated using perturbative theory, and the latter are parameterized in terms of the quark and gluon vacuum condensates. By using Cauchy's theorem, the results from QCD calculations can be matched to the hadronic channel, this is known as 'quark-hadron duality'. My Project involves using QCD Sum Rules to determine the behaviour of hadronic parameters of charmonium in the scalar and pseudoscalar channel and also light-light quark mesons in the vector and axial-vector channel at finite temperature. From our results of the behaviour of the width and the hadronic coupling at finite temperature, both channels of charmonium shows signs of survival beyond the deconfinement temperature T_c whereas the light-light quark mesons disappears at T_c. An extension of the method to finite density in the axial-vector channel of light-light quark mesons also shows signs of disappearance at the deconfinement density μ_c.

Acknowledgements

I would foremost like to thank my supervisor Professor Cesareo Dominguez for all the guidance, motivation and support he had given me for the past five years of my postgraduate studies. I could not have imagined having a better mentor for my postgraduate studies.

I must thank our collaborators Professor Marcelo Loewe, Dr Alejandro Ayala and Dr Christobal Rojas for all the insight and help they had given me during our collaboration.

Also a thank you to my colleagues Preshin Moodley, Sebastian Bodenstein and Mwande Lushozi for all the work and non-work related helps they had given me and all the fun we had together.

Lastly I must thank NIThep for funding my studies for the past five years.

Contents

1 Introduction

The method of QCD sum rules was developed in the late 70's by Shifman, Vainstein and Zakharov [1] and over the years it has been proven to be one of the most successful quantum field theory frameworks to extract hadronic information from QCD analytically in the low and intermediate energy region. This technique is based on the Operator Product Expansion (OPE) and on Cauchy's theorem in the complex energy plane. OPE separates the short (large momenta) and long (small momenta) distance interactions where the former are calculated using perturbation theory as quarks are free at short distances, the latter are parameterized in terms of quark and gluon vacuum condensates assuming that they are related to confinement in QCD. By using the Cauchy's theorem the results from QCD calculations can be matched to the hadronic channel, this is known as quark-hadron duality. These will be discussed in more detail in Section 2.

QCD sum rules has a very wide range of applications that covers the determination of hadronic spectrum (masses, couplings and widths), electromagnetic, weak and strong form factors, quark masses and the strong coupling constant. It was first extended to finite temperature by Bochkarev and Shaposnikov in the mid 80's [2]. The finite temperature extension is based on two basic assumptions, (a) that the OPE continues to be valid, with the vacuum condensates developing a temperature dependence, and (b) that no thermal singularities appear in the complex energy plane, other than on the real axis, i.e. the notion of quark-hadron duality also remains valid. Field theory evidence in support of these assumptions was provided later in [3].

Applications of QCD sum rules at finite temperature to the light-light and heavy-light quark hadrons was made in [4][5] and showed the following scenarios. (i) As the temperature increases, hadronically stable particles develop a non-zero width, and resonance width becomes broader, diverging at the deconfinement temperature T_c. Resonance broadening at finite temperature was first proposed in [6]. (ii) Above the resonance region the continuum threshold S_0 in hadronic spectral functions, i.e. the onset of perturbative QCD (PQCD), decreases monotonically with increasing temperature. In other words, as $T \to T_c$ hadrons melt disappearing from the spectrum, which then becomes smooth. (iii) The hadronic couplings, or leptonic decay constants, approach zero as $T \to T_c$. The behaviour of these three parameters at T_c - the resonance width, continuum threshold and the hadronic coupling - will therefore serve as the indicators of whether charmonium will survive beyond T_c. It was also argued in [2] that at finite temperature besides quanta with time-like momenta which can form quark antiquark pairs, it is also possible for quanta with space-like momenta to be scattered off quarks and antiquarks in the heat bath.

In Section 3 we shall use QCD sum rules to look at the behaviour of charmonium in the scalar(χ_c) and pseudoscalar(η_c) channel in finite temperature, this is an extension of the work done on J/ψ [7]. The final results show that S_0 indeed decreases monotonically with increasing temperature and reaches the PQCD threshold $s_{th} = 4m_Q^2$, where m_Q is the charm quark mass, at T_c. The hadronic mass remains almost constant with respect to changes in temperature. By using the approximation that the mass is a constant it was found that the decay width first increases monotonically but then suddenly starts to decrease around $0.8T_c$, also the hadronic coupling is found to be increasing with the increase of temperature. All these behaviours indicates that χ_c and η_c should not disappear at T_c.

In Sections 4 and 5 we look at the light-quark axial-vector meson, the $a_1(1260)$, and the light-quark vector meson, the ρ-meson, in finite temperature. It was found that S_0 decreases with increasing temperature, the width increases and diverges at T_c and the hadronic coupling decreases and reaches zero around T_c. This

indicates that $a_1(1260)$ and the ρ-meson will disappear at T_c. The temperature dependence of the ρ-width is of importance in current experiments in dimuon production in heavy ion collisions. This effect was later confirmed by many experiments [8].

In Section 6 we extend the analysis of the $a_1(1260)$ to finite density. An expression of the quark condensate has been determined in [9] and from this we can find a deconfinement density μ_c the density at which the quark condensate decreases to zero. Due to the fact that there is no available lattice result for the gluon condensate at finite density it was decided to treat it as a parameter to be determined. By assuming a monotonically increasing width that diverges at μ_c, all three parameters S_0, the hadronic coupling and the gluon condensate were found to decrease with increase in density at a temperature of $T = 80MeV$ thus agreeing with expectations.

2 QCD Sum Rules

2.1 Operator Product Expansion (OPE)

In QCD the propagator for free particles has to be modified in some way to incorporate confinement, e.g. for the quarks:

$$\frac{1}{\not{k} - m_Q} \rightarrow \frac{1}{\not{k} - m_Q + f(k^2)}$$

where $f(k^2)$ is a term that incorporates the effects of confinement and $\lim_{k^2 \to \infty} f(k^2) \rightarrow 0$ as quarks are free at large momenta (modulo vacuum fluctuation corrections).

OPE is a way to factorize the confinement effects from those of perturbative QCD (PQCD) by expanding the correlator in terms of powers of momenta.

The correlator of two currents can be expanded into a series of local operators (we use vector currents below as an example)

$$\begin{aligned} i \int d^4x e^{iq\cdot x} \langle 0 \left| T(j_\mu(x) j_\nu^\dagger(0)) \right| 0 \rangle &= (q_\mu q_\nu - q^2 g_{\mu\nu}) \Pi(q^2)|_{QCD} \\ &= (q_\mu q_\nu - q^2 g_{\mu\nu}) \sum_{N=0} \frac{C_{2N}}{(-q^2)^N} \langle 0|O_{2N}|0\rangle, \end{aligned} \tag{2.1}$$

so that

$$\Pi(q^2)|_{QCD} = \sum_{N=0} \frac{C_{2N}}{(-q^2)^N} \langle O_{2N} \rangle. \tag{2.2}$$

$\langle 0|O_{2N}|0\rangle$ are local operators constructed from quark or gluon fields and C_{2N} are just Wilson coefficients[1][10](we have used $\langle O_{2N}\rangle$ as a shorthand for $\langle 0|O_{2N}|0\rangle$).

At $N = 0$ the operator is the unit operator associated with the perturbative contribution i.e. $\langle O_0 \rangle = I$. The coefficients C_0 are determined by solving the PQCD diagrams in figure 2.1. In our analysis at finite temperature we will only solve PQCD at the leading order as the next to leading order involves the strong coupling constant α_s which at finite temperature depends on both the momenta q^2 and the temperature T. The behaviour of $\alpha_s(q^2, T)$ at low temperatures is unknown. It is also customary to ignore radiative corrections because they are expected to be at the level of only $10 - 15\%$, and QCD sum rule results at finite temperature are not as accurate.

Terms beyond $N = 0$ are all non-perturbative effects assumed to be due to confinement. At $N = 1$, the dimension $d = 2$ term $C_2\langle O_2\rangle$ cannot be constructed from local gauge invariant operators built from quark and gluon fields. It is also shown in [12] that there is in fact no evidence for such a term at $T = 0$. At very high temperatures, though, there seems to be evidence for some $d = 2$ term [11], however as we will be working at much lower temperatures, the $d = 2$ term can therefore be safely ignored.

The next two terms in the expansion is at $N = 2$ or dimension $d = 4$ and the operator is given by

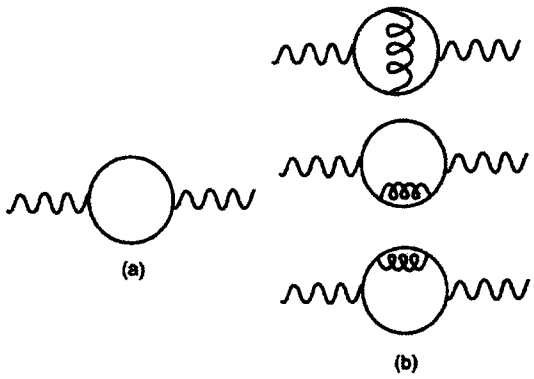

Figure 2.1: (a) Leading order (b) next to leading order diagrams in PQCD. Solid, wavy and curly lines denote quarks, currents, and gluons respectively

$$\langle O_4 \rangle = M\langle \overline{\psi}\psi \rangle + \langle G^a_{\mu\nu} G^a_{\mu\nu} \rangle \tag{2.3}$$

where ψ are quark fields, M the quark mass, $G^a_{\mu\nu}$ being the gluon fields and $a = 1, 2, ..., 8$ the gluon internal quantum numbers. The vacuum average $\langle \overline{\psi}\psi \rangle$ is known as the quark condensate and $\langle G^a_{\mu\nu} G^a_{\mu\nu} \rangle$ the gluon condensate. C_4 is determined from the diagrams in figure 2.2.

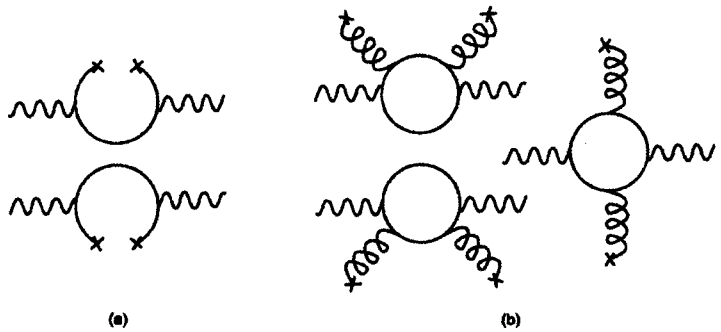

Figure 2.2: (a) Quark condensate (b) Gluon condensate diagrams. Crosses indicate interaction with the vacuum

We have assumed that confinement is due to quarks and gluons interacting with the vacuum but as we don't know how the interaction takes place, values for the quark and gluon condensate can only be obtained by fitting the theory to experimental data or by lattice QCD.

In most applications $-q^2$ is chosen large enough so that the higher dimension terms can be safely ignored.

2.2 Cauchy's Theorem and Quark-Hadron Duality

Due to confinement quarks form hadrons at low momenta so interactions between quarks and gluons can therefore be related to just interactions between hadrons. We write the correlation function for the hadronic interactions as $\Pi(s)|_{HAD}$, where $s \equiv q^2$.

The Cauchy integral theorem states that the integral of a holomorphic (differentiable everywhere) function

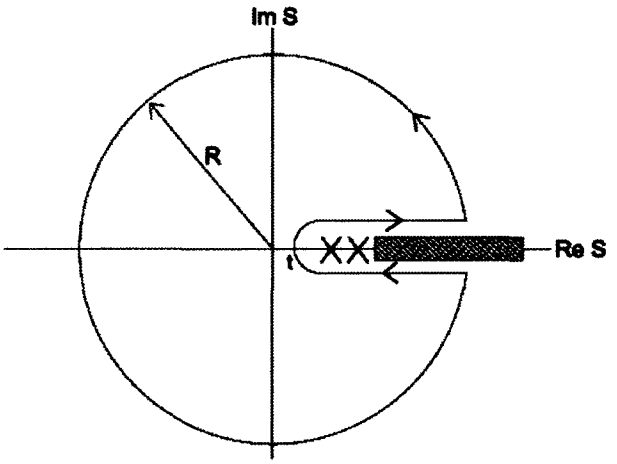

Figure 2.3: Integration contour used for hadronic correlator. Crosses indicate poles and the rectangle indicates a cut in the complex plane corresponding to the resonances.

along a closed contour in the complex plane equals zero, so if we integrate $f(s)\Pi(s)|_{HAD}$ (where $f(s)$ is also a holomorphic function) along the closed contour shown in figure 2.3 the integral is zero.

$$\begin{aligned} 0 &= \oint_C ds f(s)\Pi(s)|_{HAD} \\ 0 &= \oint_{|s|=R} ds f(s)\Pi(s)|_{HAD} + \int_t^R ds f(s)\left[\Pi(s+i\epsilon)|_{HAD} - \Pi(s-i\epsilon)|_{HAD}\right] \\ 0 &= \oint_{|s|=R} ds f(s)\Pi(s)|_{HAD} + 2i\int_t^R ds f(s)\mathrm{Im}\Pi(s)|_{HAD}. \end{aligned} \tag{2.4}$$

(to see why $\Pi(s+i\epsilon)|_{HAD} - \Pi(s-i\epsilon)|_{HAD} = 2i\mathrm{Im}\Pi(s)|_{HAD}$ see Appendix A)

If R is large enough then $\oint_{|s|=R} ds f(s)\Pi(s)|_{HAD} \to \oint_{|s|=R} ds f(s)\Pi(s)|_{PQCD}$ so

$$\oint_{|s|=R} ds f(s)\Pi(s)|_{PQCD} = -2i\int_t^R ds f(s)\mathrm{Im}\Pi(s)|_{HAD}. \tag{2.5}$$

t is a threshold at which poles and resonances can occur, for the charmonium $t = 4m_Q^2$ and for the light quark mesons $t \approx 0$.

Now we do the same contour integral for $\Pi(s)|_{QCD}$, this yields

$$\oint_{|s|=R} ds f(s)\mathrm{I}\!\Pi(s)|_{PQCD} = -2i\int_t^R ds f(s)\mathrm{Im}\mathrm{I}\!\Pi(s)|_{QCD}. \tag{2.6}$$

Equating (2.5) to (2.6) we get

$$\int_t^R ds f(s)\mathrm{Im}\Pi(s)|_{QCD} = \int_t^R ds f(s)\mathrm{Im}\Pi(s)|_{HAD}. \tag{2.7}$$

which is known as the 'Quark-Hadron Duality'.

3 (Pseudo)Scalar Charmonium in Finite Temperature QCD

3.1 Sum Rules

For the case of heavy quarks we shall use a slightly different version of the sum rules.

Using the same integration contour as in figure 2.3 but with $f(s) = \frac{1}{s+Q^2}$, then Cauchy's integration theorem gives

$$\begin{aligned}\Pi(Q^2) &= \frac{1}{2\pi i}\oint_C ds \frac{\Pi(s)}{s+Q^2} \\ &= \frac{1}{2\pi i}\oint_{|s|=R} ds \frac{\Pi(s)}{s+Q^2} + \frac{1}{\pi}\int_t^R \frac{ds}{s+Q^2}\mathrm{Im}\Pi(s)\end{aligned}$$

where $Q^2 \geq 0$ is an external four-momentum squared which is to be treated as a free parameter (it is not zero on the l.h.s because of the pole at $s = -Q^2$).

Taking $R \to \infty$, the integral over the circle should tend to zero if the correlation function vanishes fast enough. If it does not vanish it will just be a constant term so

$$\Pi(Q^2) = \frac{1}{2\pi i}\int_t^R \frac{ds}{s+Q^2}\mathrm{Im}\Pi(s) + C. \tag{3.1.1}$$

We can get rid of the constant term very easily simply by taking derivatives, for this we apply the Hilbert transformation

$$\begin{aligned}M_n(Q^2) &\equiv \frac{1}{(n+1)!}\left(-\frac{d}{dQ^2}\right)^{(n+1)}\Pi(Q^2) \\ &= \frac{1}{\pi}\int_0^\infty \frac{ds}{(s+Q^2)^{n+2}}\mathrm{Im}\Pi(s) \quad n = 1, 2, 3, ...\end{aligned} \tag{3.1.2}$$

Applying the above derivation to both the QCD and Hadronic correlators gives the quark-hadron duality relation

$$M_n(Q^2)|_{HAD} = M_n(Q^2)|_{QCD}. \tag{3.1.3}$$

The reason why the kernel $f(s) = \frac{1}{s+Q^2}$ is used here is because it will quench contributions from excited hadronic states (large s) on the l.h.s of (3.1.3), thereby allowing us to concentrate only on the ground-state mesons.

The QCD part is just the sum of perturbative QCD (PQCD) plus non-perturbative (NPQCD) higher order terms in the OPE.

$$\begin{aligned}M_n(Q^2)|_{QCD} &= M_n(Q^2)\big|_{PQCD} + M_n(Q^2)\big|_{NPQCD} \\ &= \frac{1}{\pi}\int_{4m_Q^2}^\infty \frac{ds}{(s+Q^2)^{n+2}}\,\mathrm{Im}\Pi(s)|_{PQCD} + M_n(Q^2)\big|_{NPQCD}.\end{aligned} \tag{3.1.4}$$

The hadronic part is the sum of the resonance(s) contribution followed by a continuum approximated by PQCD above a threshold S_0

$$\begin{aligned} M_n(Q^2)|_{HAD} &= M_n(Q^2)\big|_{RES} + M_n(Q^2)\big|_{PQCD} \\ &= \frac{1}{\pi}\int_{4m_Q^2}^{S_0} \frac{ds}{(s+Q^2)^{n+2}}\,\mathrm{Im}\Pi(s)|_{RES} + \frac{1}{\pi}\int_{S_0}^{\infty} \frac{ds}{(s+Q^2)^{n+2}}\,\mathrm{Im}\Pi(s)|_{PQCD}\,. \end{aligned} \tag{3.1.5}$$

Using the duality relation (3.1.3) we obtain

$$\begin{aligned} &\frac{1}{\pi}\int_{4m_Q^2}^{S_0} \frac{ds}{(s+Q^2)^{n+2}}\,\mathrm{Im}\Pi(s)|_{RES} + \frac{1}{\pi}\int_{S_0}^{\infty} \frac{ds}{(s+Q^2)^{n+2}}\,\mathrm{Im}\Pi(s)|_{PQCD} \\ &= \frac{1}{\pi}\int_{4m_Q^2}^{\infty} \frac{ds}{(s+Q^2)^{n+2}}\,\mathrm{Im}\Pi(s)|_{PQCD} + M_n(Q^2)\big|_{NPQCD}\,, \end{aligned} \tag{3.1.6}$$

rearranging we can get an expression for $M_n(Q^2)\big|_{RES}$ in terms of the PQCD and NPQCD terms

$$\frac{1}{\pi}\int_{4m_Q^2}^{S_0} \frac{ds}{(s+Q^2)^{n+2}}\,\mathrm{Im}\Pi(s)|_{RES} = \frac{1}{\pi}\int_{4m_Q^2}^{S_0} \frac{ds}{(s+Q^2)^{n+2}}\,\mathrm{Im}\Pi(s)|_{PQCD} + M_n(Q^2)\big|_{NPQCD}\,. \tag{3.1.7}$$

3.2 Correlator at $T = 0$

3.2.1 Pseudoscalar

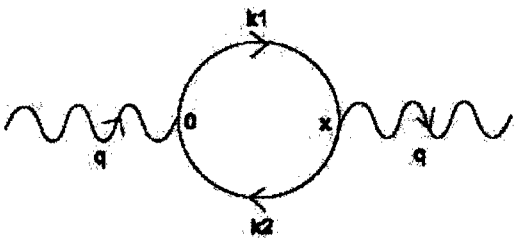

The correlator of pseudoscalar particles at zero-temperature is

$$\Pi_5(q^2) = i\int d^4x e^{iq\cdot x}\left\langle 0\left|T(J_5(x)J_5^\dagger(0))\right|0\right\rangle \tag{3.2.1}$$

where $J_5(x) = i\bar{c}^a(x)\gamma_5 c^a(x)$ and $c^a(x)$ are the charm quark fields. $a = 1,2,3$ are the colour indices.

$$\begin{aligned} T(J_5(x)J_5^\dagger(0)) &= -i^2\bar{c}_i^a(x)(\gamma_5)_{ij}c_j^a(x)\bar{c}_k^b(0)(\gamma_5)_{kl}c_l^b(0) \\ &= [iS_F(-x)]_{li}\,\delta^{ab}(\gamma_5)_{ij}\,[iS_F(x)]_{jk}\,\delta^{ab}(\gamma_5)_{kl} \\ &= -N_c\mathrm{Tr}\left[\gamma_5 S_F(x)\gamma_5 S_F(-x)\right] \end{aligned} \tag{3.2.2}$$

$N_c = 3$ are the number of colours.

Fourier transforming $\mathrm{Tr}\,[\gamma_5 S_F(x)\gamma_5 S_F(-x)]$ to k-space we get

$$\begin{aligned}\left\langle 0\left|T(J_5(x)J_5^\dagger(0))\right|0\right\rangle &= -N_c\int\frac{d^4k_1}{(2\pi)^4}e^{-ik_1\cdot x}\int\frac{d^4k_2}{(2\pi)^4}e^{ik_2\cdot x}\frac{\mathrm{Tr}\,[\gamma_5(\not{k}_1+m_Q)\gamma_5(\not{k}_2+m_Q)]}{(k_1^2-m_Q^2)(k_2^2-m_Q^2)}\\ &= -N_c\int\frac{d^4k_1}{(2\pi)^4}e^{-ik_1\cdot x}\int\frac{d^4k_2}{(2\pi)^4}e^{ik_2\cdot x}\frac{\mathrm{Tr}\left[-\not{k}_1\not{k}_2\gamma_5^2+m_Q^2\gamma_5^2\right]}{(k_1^2-m_Q^2)(k_2^2-m_Q^2)}\\ &= N_c\int\frac{d^4k_1}{(2\pi)^4}e^{-ik_1\cdot x}\int\frac{d^4k_2}{(2\pi)^4}e^{ik_2\cdot x}\frac{4(k_1\cdot k_2-m_Q^2)}{(k_1^2-m_Q^2)(k_2^2-m_Q^2)}.\end{aligned}\tag{3.2.3}$$

Substitute (3.2.3) into (3.2.1)

$$\Pi_5(q^2) = 4iN_c\int\frac{d^4k_1}{(2\pi)^4}\int\frac{d^4k_2}{(2\pi)^4}\int d^4x e^{iq\cdot x}e^{-ik_1\cdot x}e^{ik_2\cdot x}\frac{k_1\cdot k_2-m_Q^2}{(k_1^2-m_Q^2)(k_2^2-m_Q^2)}\tag{3.2.4}$$

and because $\int d^4x e^{iq\cdot x}e^{-ik_1\cdot x}e^{ik_2\cdot x} = (2\pi)^4\delta^{(4)}(q+k_2-k_1)$, (3.2.4) becomes

$$\Pi_5(q^2) = 4iN_c\int\frac{d^4k_1}{(2\pi)^4}\int\frac{d^4k_2}{(2\pi)^4}(2\pi)^4\delta^{(4)}(q+k_2-k_1)\frac{k_1\cdot k_2-m_Q^2}{(k_1^2-m_Q^2)(k_2^2-m_Q^2)}.\tag{3.2.5}$$

Integrating (3.2.5) in k_2 and rename $k_1 \equiv k$ we finally get

$$\Pi_5(q^2) = 4iN_c\int\frac{d^4k}{(2\pi)^4}\frac{1}{(k-q)^2-m_Q^2}\frac{1}{k^2-m_Q^2}(k^2-q\cdot k-m_Q^2).\tag{3.2.6}$$

As we will only be needing the imaginary part of Π_5, so by using the prescription

$$\begin{aligned}\mathrm{Im}\left[\frac{1}{(k-q)^2-m_Q^2}\frac{1}{k^2-m_Q^2}\right] &= \frac{1}{2i}\mathrm{Disc}\left[\frac{1}{(k-q)^2-m_Q^2}\right]\mathrm{Disc}\left[\frac{1}{k^2-m_Q^2}\right]\\ &= \frac{1}{2i}(-2\pi i)^2\delta[(k-q)^2-m_Q^2]\delta[k^2-m_Q^2]\end{aligned}$$

the imaginary part of Π_5 is then

$$\begin{aligned}\mathrm{Im}\Pi_5(q^2) &= -\frac{N_c}{2\pi^2}\int d^4k(k^2-k\cdot q-m_Q^2)\delta[(k-q)^2-m_Q^2]\delta[k^2-m_Q^2]\\ &= -\frac{N_c}{2\pi^2}\int d^4k(k^2-k\cdot q-m_Q^2)\left\{\delta^{(+)}[(k-q)^2-m_Q^2]+\delta^{(-)}[(k-q)^2-m_Q^2]\right\}\\ &\times\left\{\delta^{(+)}[k^2-m_Q^2]+\delta^{(-)}[k^2-m_Q^2]\right\},\end{aligned}\tag{3.2.7}$$

where $\delta^{(\pm)}[(k-q)^2-m_Q^2] \equiv \delta[(k-q)^2-m_Q^2]\Theta[\pm(q_0-k_0)]$ and $\delta^{(\pm)}[k^2-m_Q^2] \equiv \delta[k^2-m_Q^2]\Theta(\pm k_0)$.

We will now go on to show that the $\delta^{(-)}$ terms have no support in the time-like region.

$$\begin{aligned}&\int d^4k\delta[(k-q)^2-m_Q^2]\delta^{(-)}(k^2-m_Q^2)\\ &= \int\frac{d^4k}{2|k_0|}\delta[(k-q)^2-m_Q^2]\delta\left(k_0+\sqrt{|\vec{k}|^2+m_Q^2}\right)\\ &= \int\frac{d^3k}{2\sqrt{|\vec{k}|+m_Q^2}}\delta\left[q^2+2q_0\sqrt{|\vec{k}|^2+m_Q^2}+2|\vec{k}||\vec{q}|cos\theta\right].\end{aligned}$$

Since $-1 \leq cos\theta \leq 1$ which implies

$$-1 \leq \frac{-q^2 - 2q_0\sqrt{|\vec{k}|^2 + m_Q^2}}{2|\vec{k}||\vec{q}|} \leq 1,$$

by looking at the lower limit we see that

$$\begin{aligned} -q^2 - 2q_0\sqrt{|\vec{k}|^2 + m_Q^2} &\geq -2|\vec{k}||\vec{q}| \\ -q^2 &\geq 2|\vec{k}|\left(q_0\sqrt{1 + \frac{m_Q^2}{|\vec{k}|^2}} - |\vec{q}|\right) \\ |\vec{k}| &\leq \frac{-q^2}{2\left(q_0\sqrt{1 + \frac{m_Q^2}{|\vec{k}|^2}} - |\vec{q}|\right)}. \end{aligned} \tag{3.2.8}$$

Since $q^2 > 0$ the right hand side of (3.2.8) is less than zero, this creates a contradiction because $|\vec{k}|$ must be positive, so we conclude that there is no support for $\delta^{(-)}(k^2 - m_Q^2)$.

There is also no support for $\delta^{(-)}[(k-q)^2 - m_Q^2]$ because $k_0 < q_0$, this is explained in the end of Appendix A.

(3.2.7) now becomes

$$\mathrm{Im}\Pi_5(q^2) = -\frac{N_c}{2\pi^2}\int d^4k(k^2 - k\cdot q - m_Q^2)\delta^{(+)}[(k-q)^2 - m_Q^2]\delta^{(+)}[k^2 - m_Q^2]. \tag{3.2.9}$$

To compute (3.2.9) we use the solutions for the following phase space integrals which can be found in [13]

$$\begin{aligned} \int d^4k\delta^{(+)}\left[(k-q)^2 - m_Q^2\right]\delta^{(+)}\left[k^2 - m_Q^2\right] &= \frac{\pi}{2}\Theta(q^0)\Theta(q^2 - 4m_Q^2)v \\ \int d^4k\delta^{(+)}\left[(k-q)^2 - m_Q^2\right]\delta^{(+)}\left[k^2 - m_Q^2\right]k^2 &= \frac{\pi}{2}\Theta(q^0)\Theta(q^2 - 4m_Q^2)m_Q^2 v \\ \int d^4k\delta^{(+)}\left[(k-q)^2 - m_Q^2\right]\delta^{(+)}\left[k^2 - m_Q^2\right]k_\mu &= \frac{\pi}{4}\Theta(q^0)\Theta(q^2 - 4m_Q^2)vq_\mu \end{aligned} \tag{3.2.10}$$

where $v = \sqrt{1 - \frac{4m_Q^2}{q^2}}$. The Θ functions will be omitted, all results will be understood as $q^0 > 0$ and $q^2 > 4m_Q^2$.

Substituting (3.2.10) into (3.2.9) we finally get

$$\begin{aligned} \mathrm{Im}\Pi_5(q^2) &= -\frac{N_c}{2\pi^2}\left(\frac{\pi}{2}m_Q^2 v - \frac{\pi}{4}vq^2 - \frac{\pi}{2}m_Q^2 v\right) \\ &= \frac{3}{8\pi}vq^2. \end{aligned} \tag{3.2.11}$$

3.2.2 Scalar

For scalar particles the correlator is

$$\Pi_s(q^2) = i\int d^4x e^{iq\cdot x}\left\langle 0\left|T(J_s(x)J_s^\dagger(0))\right|0\right\rangle \tag{3.2.12}$$

and

$$\begin{aligned} T(J_s(x)J_s^\dagger(0)) &= \bar{c}_i^a(x)(\mathbf{1})_{ij}c_j^a(x)\bar{c}_k^b(0)(\mathbf{1})_{kl}c_l^b(0) \\ &= -\left[iS_F(-x)\right]_{li}\delta^{ab}(\mathbf{1})_{ij}\left[iS_F(x)\right]_{jk}\delta^{ab}(\mathbf{1})_{kl} \\ &= N_c\mathrm{Tr}\left[S_F(x)S_F(-x)\right]. \end{aligned} \tag{3.2.13}$$

Following a similar calculation as for the pseudoscalar we get

$$\mathrm{Im}\Pi_s(q^2) = \frac{3}{8\pi} v^3 q^2. \tag{3.2.14}$$

3.3 Correlator at $T \neq 0$

3.3.1 Time-Like Region $q^2 > 4m_Q^2$

At finite temperature the virtual quanta with time-like momenta $q^2 > 4m_Q^2$ in matter consisting of free fermions with distribution $n_F(|E|)$ ($n_F(Z) \equiv (1+e^{Z/T})^{-1}$) are converted into quark-antiquark pair at a rate proportional to $[1-n_F(|k_1|)][1-n_F(|k_2|)]$ according to Pauli's principle. At the same time quanta are produced in the matter at a rate proportional to $n_F(|k_1|)n_F(|k_2|)$ [2]. For the pseudoscalar particle, the rate of disappearence of time-like quanta in the medium is

$$\begin{aligned}\Pi_5(q^2,T) &= i\int d^4x e^{iq\cdot x}\left\langle 0\left|T(J_5(x)J_5^\dagger(0))\right|0\right\rangle \{[1-n_F(|k_1|)][1-n_F(|k_2|)] - n_F(|k_1|)n_F(|k_2|)\} \\ &= iN_c\int\frac{d^4k}{(2\pi)^4}\mathrm{Tr}\left[S_F(k)\gamma_5 S_F(k-q)\gamma_5\right]\{1-n_F(|k_0|)-n_F(|k_0-q_0|)\}. \end{aligned}\tag{3.3.1}$$

The imaginary part of $\Pi_5(T)$ is

$$\begin{aligned}\mathrm{Im}\Pi_5(q^2,T) = -8N_c\pi^2\int\frac{d^4k}{(2\pi)^4}\,&(k^2-q\cdot k-m_Q^2) \\ &\times\{1-n_F(|k_0|)-n_F(|k_0-q_0|)\}\,\delta^{(+)}(k^2-m_Q^2)\delta^{(+)}([(k-q)^2-m_Q^2]\end{aligned}\tag{3.3.2}$$

for which we used the same reasoning as in section 3 for the fact that there are no support for $\delta^{(-)}(k^2-m_Q^2)$ and $\delta^{(-)}[(k-q)^2-m_Q^2]$.

(A more rigorous derivation of (3.3.2) is given in Appendix C)

By using the thermal phase space integral determined in Appendix B for the rest frame of the thermal bath (i.e. limit $|\vec{q}|\to 0$) we get

$$\begin{aligned}\mathrm{Im}\Pi_5(\omega^2,T) &= \frac{3}{8\pi}v\omega^2\left[1-2n_F\left(\left|\frac{\omega}{2}\right|\right)\right] \\ &\equiv \frac{3}{16\pi}\omega^2\int_{-v}^{v}dx\left[1-2n_F\left(\left|\frac{\omega}{2}\right|\right)\right].\end{aligned}\tag{3.3.3}$$

where $v=\sqrt{1-\frac{4m_Q^2}{\omega^2}}$ and $\omega\equiv k_0$.

Following a similar procedure as above we get for the scalar particle

$$\begin{aligned}\mathrm{Im}\Pi_s(\omega^2,T) &= \frac{3}{8\pi}v^3\omega^2\left[1-2n_F\left(\left|\frac{\omega}{2}\right|\right)\right] \\ &\equiv \frac{9}{16\pi}\omega^2\int_{-v}^{v}x^2dx\left[1-2n_F\left(\left|\frac{\omega}{2}\right|\right)\right].\end{aligned}\tag{3.3.4}$$

3.3.2 Space-Like Region $q^2 < 4m_Q^2$

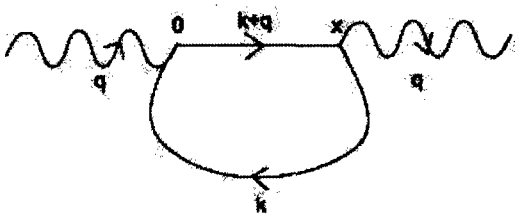

At zero temperature this term is not present as in a vacuum there are no particles for the quanta to scatter from, but at finite temperature (in a heat bath), quanta with space-like momenta $q^2 < 0$ may be absorbed by the quarks and antiquarks in the medium at a rate of $n_F(|k_0|)[1 - n_F(|q_0 + k_0|)]$ and then reemitted at a rate of $n_F(|q_0 + k_0|)[1 - n_F(|k_0|)]$ [2]. The rate at which space-like quanta disappear for pseudoscalar particles is then

$$\Pi_5^{(s)}(q^2,T) = iN_c \int \frac{d^4k}{(2\pi)^4} \mathrm{Tr}\left[S_F(k)\gamma_5 S_F(q+k)\gamma_5\right] \{n_F(|k_0|)[1 - n_F(|q_0 + k_0|)] - n_F(|q_0 + k_0|)[1 - n_F(|k_0|)]\}. \tag{3.3.5}$$

Following the calculations from the paper by Bochkarev and Shaposhnikov [2] it is found that $\mathrm{Im}\Pi_s(q^2,T)$ (given by $\mathrm{Im}\Pi_{00}(q^2,T)_s/|\vec{q}|^2$) is

$$\mathrm{Im}\Pi_5^{(s)}(q^2,T) = \frac{3}{16\pi} q^2 \int_v^\infty dx \Delta n_F(x) \tag{3.3.6}$$

where $v = \sqrt{1 - \frac{4m_Q^2}{q^2}}$ and $\Delta n_F(x) \equiv n_F\left(\frac{|\vec{q}|x+\omega}{2}\right) - n_F\left(\frac{|\vec{q}|x-\omega}{2}\right)$.

By noting that $q^2 = (\omega^2 - |\vec{q}|^2) < 0$ therefore as $|\vec{q}| \to 0$, ω will also go to zero, so in the rest frame of the thermal bath, we see that $\Delta n_F(x)$ simply becomes a total derivative

$$\begin{aligned} \Delta n_F(x) &= \omega \frac{d}{d\left(\frac{|\vec{q}|x}{2}\right)} n_F\left(\frac{|\vec{q}|x}{2}\right) \\ &= \frac{2\omega}{|\vec{q}|} \frac{d}{dx} n_F\left(\frac{|\vec{q}|x}{2}\right). \end{aligned} \tag{3.3.7}$$

(3.3.6) is now

$$\mathrm{Im}\Pi_5^{(s)}(q^2,T) = \frac{3}{8\pi} q^2 \frac{\omega}{|\vec{q}|} \int_v^\infty dx \frac{d}{dx} n_F\left(\frac{|\vec{q}|x}{2}\right), \tag{3.3.8}$$

integrating by parts yields

$$\mathrm{Im}\Pi_5^{(s)}(q^2,T) = -\frac{3}{4\pi} q^2 \frac{\omega}{|\vec{q}|} n_F\left(\frac{|\vec{q}|v}{2}\right). \tag{3.3.9}$$

Lastly by and noting that

$$\lim_{|\vec{q}|,\omega\to 0} q^2 \frac{\omega}{|\vec{q}|} = \lim_{|\vec{q}|,\omega\to 0} (\omega^2 - |\vec{q}|^2) \frac{\omega}{|\vec{q}|} \to 0$$

we see that

$$\lim_{|\vec{q}|,\omega\to 0} \mathrm{Im}\Pi_5^{(s)}(q^2,T) \to 0. \tag{3.3.10}$$

For the scalar correlator we have

$$\mathrm{Im}\Pi_s^{(s)}(q^2,T) = \frac{9}{16\pi}q^2\int_v^\infty x^2 dx \Delta n_F(x), \tag{3.3.11}$$

and following a similar procedure up to (3.3.9) we get

$$\mathrm{Im}\Pi_s^{(s)}(q^2,T) = -\frac{9}{8\pi}q^2\frac{\omega}{|\vec{q}|}\left[v^2 n_F\left(\frac{|\vec{q}|v}{2}\right) + 2\int_v^\infty x n_F\left(\frac{|\vec{q}|x}{2}\right)dx\right]. \tag{3.3.12}$$

By performing a change of variables $y = \frac{|\vec{q}|x}{2}$ (3.3.12) simplifies to

$$\mathrm{Im}\Pi_s^{(s)}(q^2,T) = -\frac{9}{8\pi}q^2\frac{\omega}{|\vec{q}|}\left[v^2 n_F\left(\frac{|\vec{q}|v}{2}\right) + \frac{8}{|\vec{q}|^2}\int_{\frac{|\vec{q}|v}{2}}^\infty y n_F(y)\,dy\right]. \tag{3.3.13}$$

Lastly by making the approximation that $\omega << |\vec{q}|$ and noting that

$$\lim_{|\vec{q}|,\omega\to 0}\int_0^{|\vec{q}|^2}\frac{\omega}{|\vec{q}|^3}d\omega^2 = \frac{2}{3}\int_0^{|\vec{q}|^2}\delta(\omega^2)d\omega^2,$$

$$\lim_{|\vec{q}|,\omega\to 0}\frac{|\vec{q}|v}{2} = \frac{|\vec{q}|}{2}\sqrt{1+\frac{4m_Q^2}{|\vec{q}|^2-\omega^2}} \to m_Q$$

we get the final expression

$$\begin{aligned}\mathrm{Im}\Pi_s^{(s)}(q^2,T) &= -\frac{9}{2\pi}q^2\frac{\omega}{|\vec{q}|^3}\left[m_Q^2 n_F(m_Q) + 2\int_{m_Q}^\infty y n_F(y)\,dy\right] \\ &= -\frac{3}{\pi}q^2\delta(\omega^2)\left[m_Q^2 n_F(m_Q) + 2\int_{m_Q}^\infty y n_F(y)\,dy\right].\end{aligned} \tag{3.3.14}$$

The Hilbert moment for (3.3.14) is

$$\begin{aligned}M_n(Q^2,T)_s|_{PQCD}^{q^2<0} &= \frac{3}{\pi^2}\int_0^{S_0(T)}\frac{d\omega^2}{(\omega^2+Q^2)^{n+2}}q^2\delta(\omega^2)\left[m_Q^2 n_F(m_Q) + 2\int_{m_Q}^\infty y n_F(y)dy\right] \\ &= \frac{2}{\pi^2}\frac{|\vec{q}|^2}{(Q^2)^{n+2}}\left[m_Q^2 n_F(m_Q) + 2\int_{m_Q}^\infty y n_F(y)dy\right]\end{aligned} \tag{3.3.15}$$

which in the limit $|\vec{q}| \to 0$ vanishes.

So there are no space-like region contributions in the FESR for both the pseudoscalar and scalar particles.

3.4 Condensates

Due to the large mass of heavy quarks being far off-shell at the momentum scale Λ_{vac}, the heavy quark condensate is heavily suppressed. We shall therefore not consider the heavy quark condensate term in the analysis. [1][10]

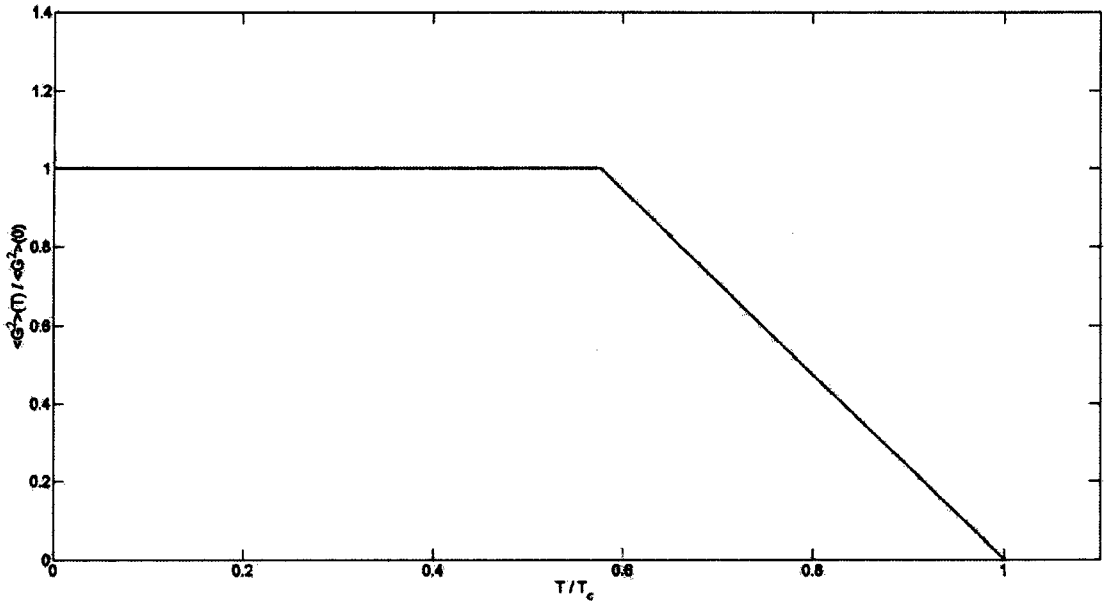

Figure 3.1: Plot of $\frac{\left\langle \frac{\alpha_s}{\pi} G^2 \right\rangle (T)}{\left\langle \frac{\alpha_s}{\pi} G^2 \right\rangle (0)}$ against $\frac{T}{T_c}$.

The Hilbert moment of the Gluon-Condensate is given in [14], for the pseudoscalar case it is

$$M_n(Q^2,T)_5\big|_{GC} = -\frac{3}{8\pi^2}\frac{2^{(n+1)}n!}{(4m_Q^2)^{(n+1)}}\frac{1}{(1+\xi)^{n+2}}\frac{(n+1)(n+2)(n+3)(n+4)}{(2n+5)(2n+3)!!} \times \left[F\left(n+2,-\frac{3}{2},n+\frac{7}{2};\rho\right) - \frac{6}{n+4}F\left(n+2,-\frac{1}{2},n+\frac{7}{2};\rho\right)\right]\Phi \tag{3.4.1}$$

and for the scalar it is

$$M_n(Q^2,T)_s\big|_{GC} = -\frac{27}{8\pi^2}\frac{2^{(n+1)}n!}{(4m_Q^2)^{(n+1)}}\frac{1}{(1+\xi)^{n+2}}\frac{(n+1)(n+2)(n+3)(n+4)}{(2n+7)(2n+5)!!} \times \left[F\left(n+2,-\frac{1}{2},n+\frac{9}{2};\rho\right) - \frac{2}{3(n+4)}F\left(n+2,\frac{1}{2},n+\frac{9}{2};\rho\right)\right]\Phi \tag{3.4.2}$$

where

$$F(a,b,c;z) = \sum_{n=0}^{\infty}\frac{(a)_n(b)_n}{(c)_n}\frac{z^n}{n!} \quad \text{with} \quad (a)_n = a(a+1)(a+2)...(a+n-1)$$

is the hypergeometric function and

$$\xi \equiv \frac{Q^2}{4m_Q^2} \quad ; \quad \rho \equiv \frac{\xi}{1+\xi} \quad ; \quad \Phi \equiv \frac{4\pi^2}{9}\frac{1}{(4m_Q^2)^2}\left\langle \frac{\alpha_s}{\pi}G^2\right\rangle_T$$

From the results of lattice QCD [15], to a reasonable accuracy $\left\langle \frac{\alpha_s}{\pi}G^2\right\rangle$ at finite temperature can be approximated by

$$\left\langle \frac{\alpha_s}{\pi}G^2\right\rangle_T = \left\langle \frac{\alpha_s}{\pi}G^2\right\rangle_0 \left[\Theta(T^*-T) + \frac{T_c^*-T}{T_c^*-T^*}\Theta(T-T^*)\right] \tag{3.4.3}$$

where $\left\langle \frac{\alpha_s}{\pi} G^2 \right\rangle_0 = \left\langle \frac{\alpha_s}{\pi} G^2 \right\rangle_T \Big|_{T=0}$, T^* is the temperature at which $\left\langle \frac{\alpha_s}{\pi} G^2 \right\rangle_T$ starts decreasing and T_c^* is the temperature at which $\left\langle \frac{\alpha_s}{\pi} G^2 \right\rangle_T$ reaches zero, $T^* \approx 150\text{MeV}$ and $T_c^* \approx 260\text{MeV}$. (3.4.3) is plotted in figure 3.1.

$\left\langle \frac{\alpha_s}{12\pi} G^2 \right\rangle_0 = 0.05 \pm 0.02\text{GeV}^4$ [17], we simply used $\left\langle \frac{\alpha_s}{12\pi} G^2 \right\rangle_0 = 0.05\text{GeV}^4$ for all the analysis in section 3.7.

We do not consider the gluonic twist-two term in the OPE introduced in [16] as we have found it to be only around 5% of $\left\langle \frac{\alpha_s}{12\pi} G^2 \right\rangle_T$, as in the case of vector charmonium (J/Ψ) [7].

3.5 Hadronic Terms

First we define the decay constant f as

$$\langle 0|J_{(5)}(0)|H(k)\rangle = fM^2, \tag{3.5.1}$$

where $H(k)$ stands for $\eta_c(\chi_c)$ and M is the mass of $\eta_c(\chi_c)$.

So for the zero width approximation the resonance term is

$$\frac{1}{\pi} \text{Im}\Pi(s)|_{RES}^{\Gamma=0} = f^2 M^2 \delta\left(s - M^2\right). \tag{3.5.2}$$

The Hilbert moment for zero width is

$$\begin{aligned} M_n(Q^2)|_{RES}^{\Gamma=0} &= \int_{4m_Q^2}^{S_0} \frac{ds}{(s+Q^2)^{n+2}} f^2 M^2 \delta(s - M^2) \\ &= \frac{f^2 M^2}{(M^2+Q^2)^{n+2}}. \end{aligned} \tag{3.5.3}$$

For finite width Γ_V we replace the delta function by a Breit-Wigner approximation

$$\delta(s - M^2) \to \frac{C}{(s-M^2)^2 + M^2\Gamma^2} \tag{3.5.4}$$

with the constant C fixed by the requirement

$$\begin{aligned} \int_0^\infty \delta(s - M^2) ds = 1 = \int_0^\infty ds \frac{C}{(s-M^2)^2 + M^2\Gamma^2} \\ = \frac{C}{M\Gamma} \tan^{-1}\left(\frac{s-M^2}{M\Gamma}\right)\Big|_0^\infty \\ \approx \frac{C\pi}{M\Gamma} \end{aligned}$$

$$\Rightarrow C \approx \frac{M\Gamma}{\pi} \tag{3.5.5}$$

where we have used the approximation that $\tan^{-1}\left(\frac{s-M^2}{M\Gamma}\right)\Big|_{s=0} \approx -\frac{\pi}{2}$ as $\Gamma << M$ for charmonium.

The Breit-Wigner parametrization of the resonance term is then

$$\frac{1}{\pi} \text{Im}\Pi(s)|_{RES}^{\Gamma>0} = \frac{1}{\pi} \frac{f^2 M^3 \Gamma}{(s-M^2)^2 + M^2\Gamma^2}, \tag{3.5.6}$$

and the Hilbert moment is

$$M_n(Q^2)|_{RES}^{\Gamma>0} = \frac{1}{\pi} f^2 M^3 \Gamma \int_{4m_Q^2}^{S_0} \frac{ds}{(s+Q^2)^{n+2}} \frac{1}{(s-M^2)^2 + M^2\Gamma^2}. \tag{3.5.7}$$

At finite temperature the only changes we need to make are changing $S_0 \to S_0(T)$, $M \to M(T)$, $\Gamma \to \Gamma(T)$ and $f \to f(T)$.

Since the current can scatter off heavy-light quark pseudoscalar mesons (D-meson) in the thermal bath therefore it is necessary to also consider hadronic scattering terms. In the case of η_c, the pseudoscalar current couples to an odd number of pseudoscalars, this effect is negligible as it is a higher order loop effect. For the scalar case we can show by performing a similar calculation as in section 3.3.2 by replacing quarks with D-mesons that it also vanishes in the limit $|\vec{q}| \to 0, \omega \to 0$.

3.6 Determination of Parameters

If we look at the Hilbert moment for the zero width resonance (3.5.3) we see that

$$\left.\frac{M_1(Q^2,T)|_{RES}}{M_2(Q^2,T)|_{RES}}\right|_{\Gamma=0} = \left.\frac{M_2(Q^2,T)|_{RES}}{M_3(Q^2,T)|_{RES}}\right|_{\Gamma=0} = M^2(T) + Q^2. \tag{3.6.1}$$

We can assume that this relation also holds for the finite width moment (3.5.7) provided the width is not too large

$$\left.\frac{M_1(Q^2,T)|_{RES}}{M_2(Q^2,T)|_{RES}}\right|_{\Gamma>0} = \left.\frac{M_2(Q^2,T)|_{RES}}{M_3(Q^2,T)|_{RES}}\right|_{\Gamma>0}. \tag{3.6.2}$$

By (3.1.3) this would also imply that

$$\frac{M_1(Q^2,T)|_{QCD}}{M_2(Q^2,T)|_{QCD}} = \frac{M_2(Q^2,T)|_{QCD}}{M_3(Q^2,T)|_{QCD}}, \tag{3.6.3}$$

and since $M_n(Q^2,T)|_{QCD}$ only depends on $S_0(T)$, we can solve for $S_0(T)$ by using a fixed Q^2.

Using the determined $S_0(T)$ we can find $M(T)$ and $\Gamma(T)$ from the relations

$$\left.\frac{M_1(Q^2,T)|_{RES}}{M_2(Q^2,T)|_{RES}}\right|_{\Gamma>0} = \frac{M_1(Q^2,T)|_{QCD}}{M_2(Q^2,T)|_{QCD}} \tag{3.6.4}$$

and

$$\left.\frac{M_1(Q^2,T)|_{RES}}{M_3(Q^2,T)|_{RES}}\right|_{\Gamma>0} = \frac{M_1(Q^2,T)|_{QCD}}{M_3(Q^2,T)|_{QCD}}. \tag{3.6.5}$$

Finally using the $S_0(T)$, $M_V(T)$ and $\Gamma_V(T)$ we found, we can determine $f(T)$ from

$$M_1(Q^2,T)|_{RES}^{\Gamma>0} = M_1(Q^2,T)|_{QCD} \tag{3.6.6}$$

3.7 Results

Using (3.6.3) and letting $Q^2 = 0$ we determined $S_0(0) = 9.1\text{GeV}^2$ for η_c, and by setting $\Gamma(0) = \Gamma|_{EXP} = 27\text{MeV}$ gives $M(0) = 2.9\text{GeV}$, to be compared to the experimental value of $M|_{EXP} = 2.98\text{GeV}$. For χ_c we got $S_0(0) = 11.6\text{GeV}^2$, and by setting $\Gamma(0) = \Gamma|_{EXP} = 10.2\text{MeV}$ gives $M(0) = 3.2\text{GeV}$, to be compared to the experimental value of $M|_{EXP} = 3.41\text{GeV}$. The decay constant was determined to be $f = 519\text{MeV}$ for η_c and $f = 606\text{MeV}$ for χ_c.

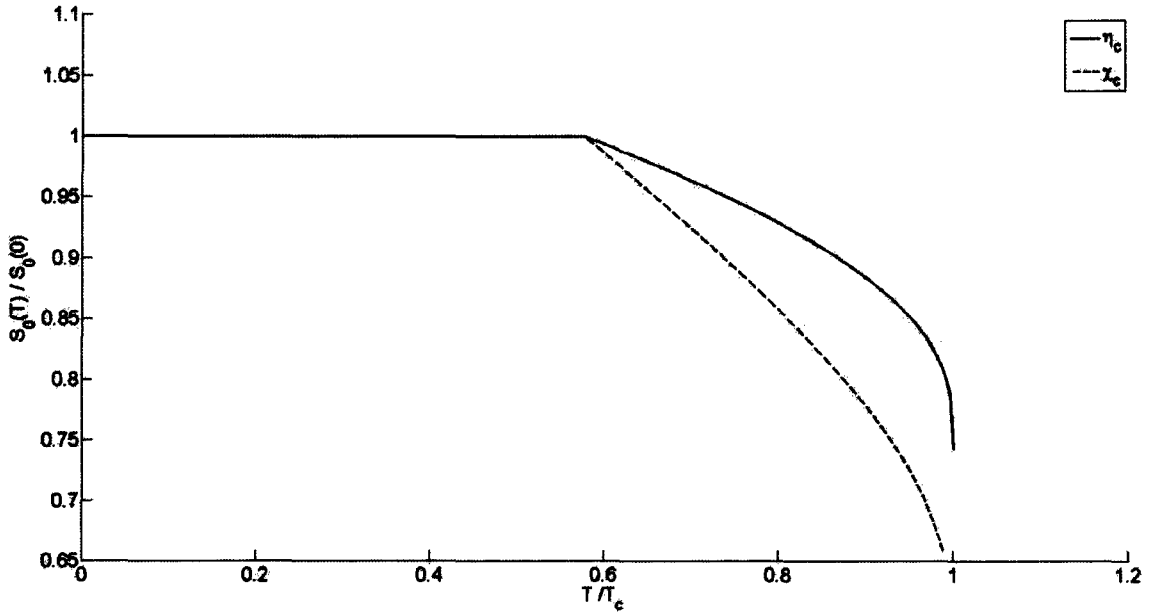

Figure 3.2: Plot of $S_0(T)/S_0(0)$ against T/T_c for η_c and χ_c

Result of $S_0(T)$ for η_c (pseudoscalar) and χ_c (scalar) in shown in figure 3.2. $S_0(T)$ stays constant up to around $0.58T_c$ then it starts to decrease and at T_c it reaches $4m_Q^2$. This behaviour is expected as when the temperature increases the QCD continuum should start occurring at lower and lower energies and eventually at some point the whole energy spectrum should consist of only the QCD continuum i.e. quark gluon plasma. This decrease of S_0 is solely caused by the decrease of the gluon condensate.

$M(T)$ and $\Gamma(T)$ are still not readily determinable from (3.6.4) and (3.6.5) because, first, the two parameters are coupled together inside an integral so they cannot be determined individually, and second, even by trying to solve for them numerically using the Newton-Raphson method for multi-variables, due to the tiny width of charmonium relative to the mass the method proves to be numerically unstable.

We therefore first assumed that $\Gamma(T)$ is small and constant then using (3.6.4) we determined $M(T)$, this is shown in figure 3.3. In figure 3.3 we see that $M(T)$ only decreased by about 5% for η_c and 14% for χ_c at T_c, we shall therefore approximate $M(T)$ as a constant with respect to temperature i.e. $M(T) \approx M(0)$.

By assuming $M(T)$ is a constant we determined $\Gamma(T)$ as shown in figure 3.4. $\Gamma(T)$ stays constant up to around $0.58T_c$ at which it starts to increase. At $0.75T_c$ for the scalar and $0.9T_c$ for the pseudoscalar the $\Gamma(T)$ reaches a maximum and then starts to decrease. At $0.96T_c$ for η_c and $0.82T_c$ for χ_c there are no more solutions as the value for $S_0(T)$ becomes lesser than M^2, the same was seen in the vector charmonium J/ψ [7]

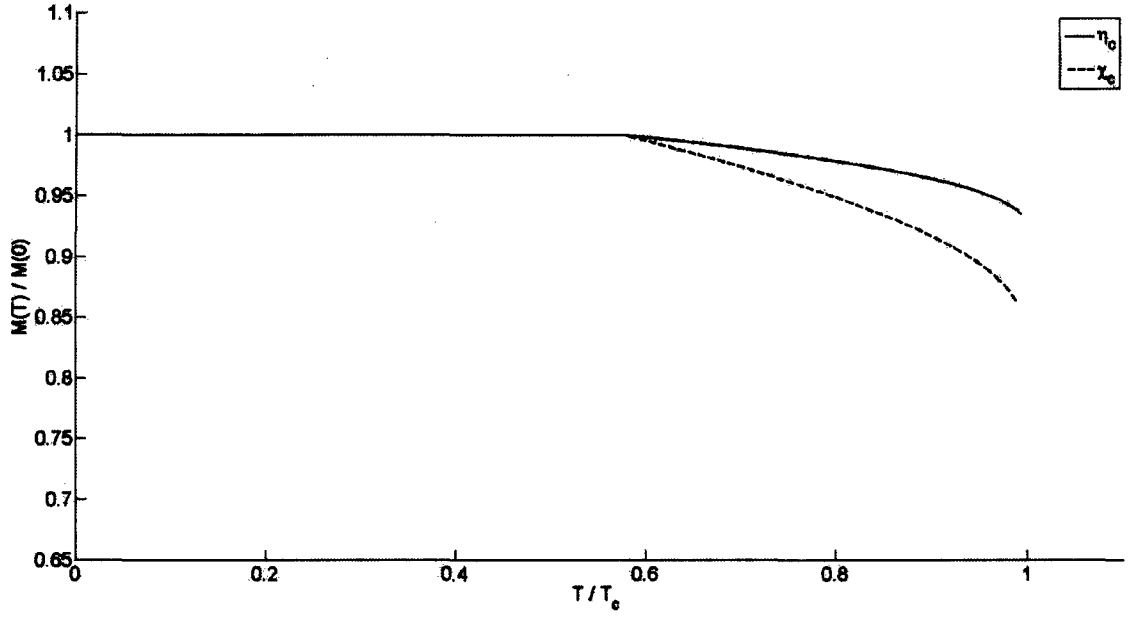

Figure 3.3: Plot of $M(T)/M(0)$ against T/T_c assuming constant $\Gamma(T)$

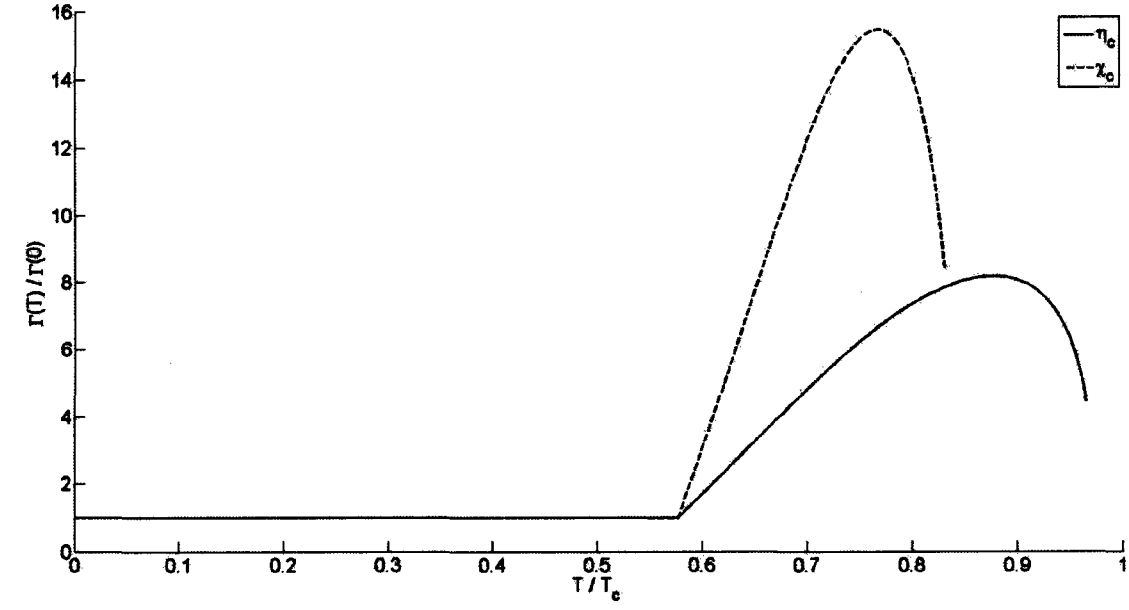

Figure 3.4: Plot of $\Gamma(T)/\Gamma(0)$ against T/T_c assuming constant mass

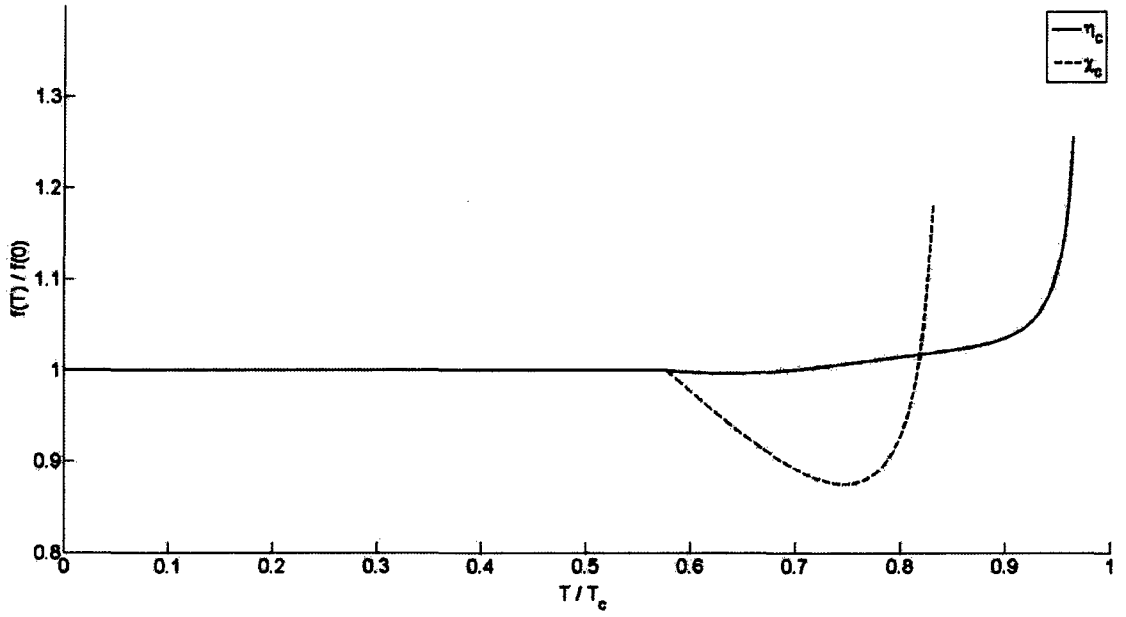

Figure 3.5: Plot of $f(T)/f(0)$ against T/T_c assuming constant mass

Finally by using $M(T)$ constant and with $S_0(T)$ and $\Gamma(T)$ already determined, we can determine $f(T)$ from (3.6.6). The result for $f(T)$ is shown in figure 3.5. We see that it stays constant till $0.58T_c$ where it first decreases a little and then increases.

The fact that $\Gamma(T)$ starts decreasing and $f(T)$ is increasing suggests that (pseudo)scalar charmonium will likely survive beyond T_c.

The above results are relatively insensitive to larger values in Q^2. Even at $Q^2 = 10\text{GeV}^2$ we still see the parameters behaving similarly to that at $Q^2 = 0$ with only slight changes (5%) to the zero temperature values.

3.8 Checking Validity of Method

3.8.1 Validity of (3.6.2)

3.8.2 Checking Validity of Method at Large Γ_V

In section 3.6 we mentioned that (3.6.2) should hold provided the width is not too large, but how large is 'too large'?

In figure 3.6 we plotted $\left[\frac{M_1|_{RES}}{M_2|_{RES}} \Big/ \frac{M_2|_{RES}}{M_3|_{RES}}\right]_{\Gamma>0}$ against S_0 for the pseudoscalar (η_c) using a fixed $M = 2.9\text{GeV}$ at various Γ. For (3.6.2) to be valid it would require $\left[\frac{M_1|_{RES}}{M_2|_{RES}} \Big/ \frac{M_2|_{RES}}{M_3|_{RES}}\right]_{\Gamma>0}$ to be as close to 1 as possible. We can see in figure 3.6 that even at a very large width of 1 GeV and $S_0 = 15\text{GeV}^2$, (3.6.2) still holds pretty well as there is only a deviation of $< 2.5\%$ from 1.

A similar behaviour is seen for χ_c.

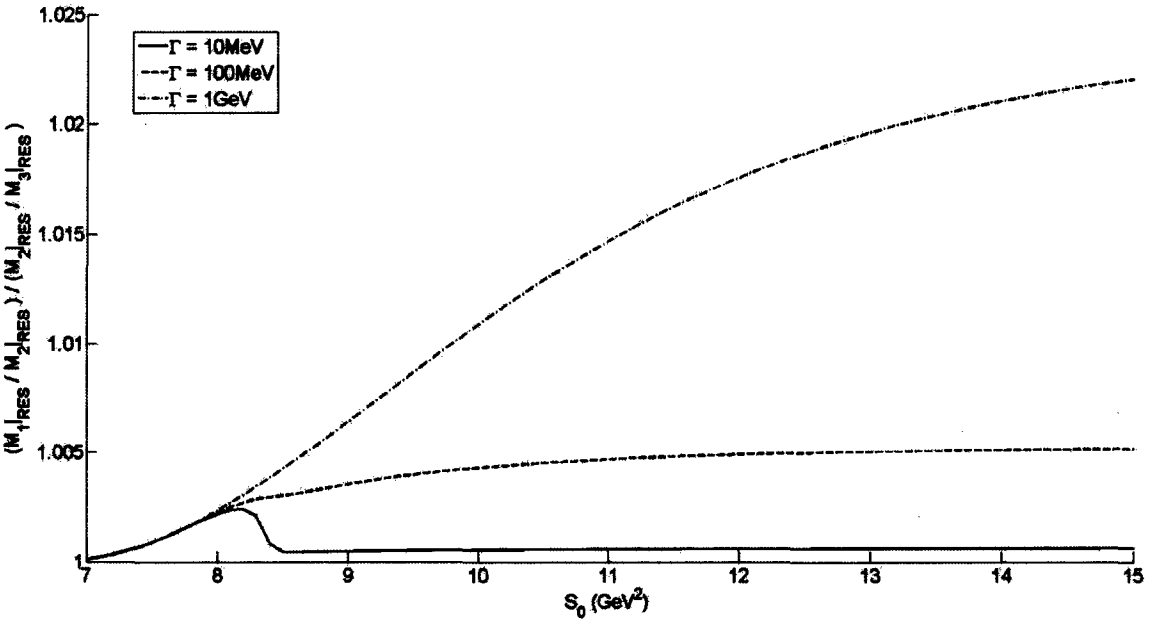

Figure 3.6: $\left[\frac{M_1|_{RES}}{M_2|_{RES}} \Big/ \frac{M_2|_{RES}}{M_3|_{RES}}\right]_{\Gamma>0}$ plotted against S_0 for η_c at different Γ.

3.8.3 Checking Validity of Constant Mass Approximation

In our determination of the width we have assumed the mass to be a constant but as seen in figure 3.3 we do actually see a decrease of 14% for χ_c so it might a good idea to check how a variable mass affects the behaviour of the width and decay constant.

For the following analysis I have defined the mass to be

$$M^{mod}(T) = A[M(T) - M(0)] + M(0) \tag{3.8.1}$$

where $M(T)$ is the mass determined in figure 3.3 and $0 < A < 1$ is a constant factor which adjusts how fast the mass decreases. If $A = 0$ then $M^{mod}(T) = M(0)$ and if $A = 1$ then $M^{mod}(T) = M(T)$. The results for the width and coupling of χ_c for the cases of $A = 0, 0.3, 0.5, 0.8$ is shown in the figures 3.7 and 3.8.

We see that as A increases the behaviour of $\Gamma(T)$ and $f(T)$ is still similar to that of $A = 0$ where $\Gamma(T)$ first increases then decreases and vice versa for $f(T)$, the only difference is that this change from increasing to decreasing $\Gamma(T)$ or decreasing to increasing $f(T)$ just happens at higher temperatures. A similar behaviour is observed for η_c.

From this we can conclude that it is reasonable to use a constant mass approximation when determining $\Gamma(T)$ and $f(T)$.

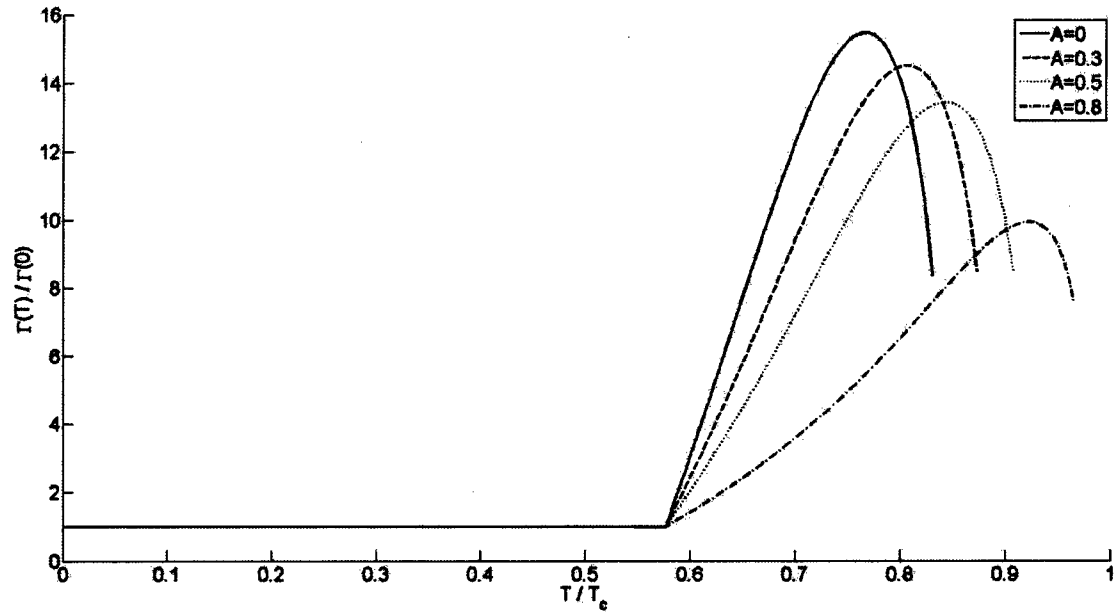

Figure 3.7: $\Gamma(T)/\Gamma(0)$ plotted against T/T_c for χ_c at different values of A.

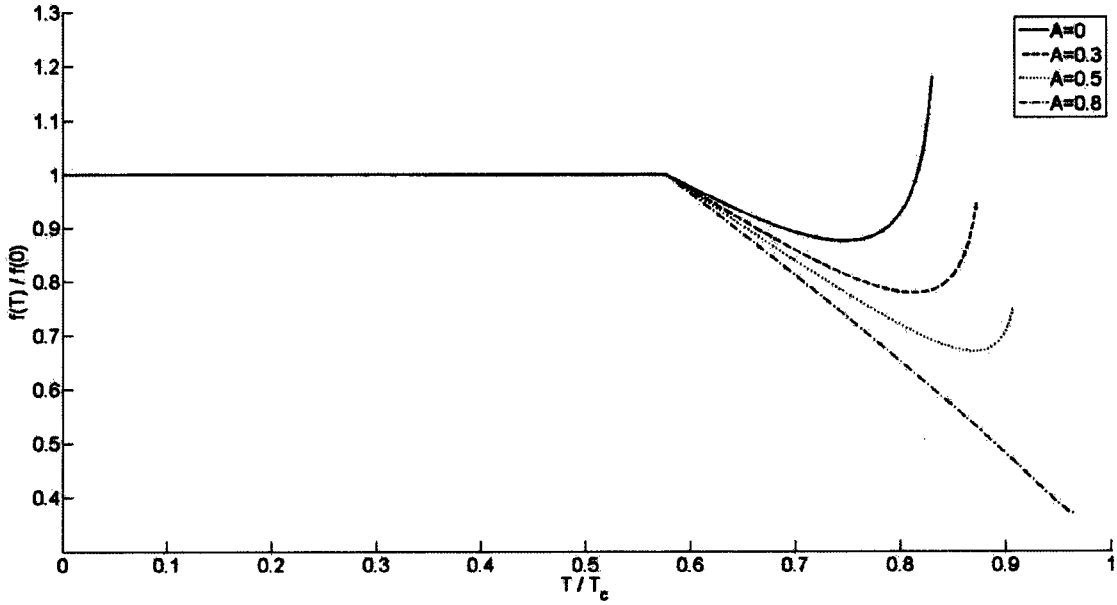

Figure 3.8: $f(T)/f(0)$ plotted against T/T_c for χ_c at different values of A.

3.9 Conclusion

Using a QCD sum rule approach we have determined the behaviour of the hadronic parameters of charmonium in the (pseudo)scalar channels, η_c and χ_c, at finite temperature. Due to the absence of the quark condensate in the OPE, the gluon condensate becomes the leading term in the OPE, and thus solely responsible for the temperature behaviour of η_c and χ_c. The continuum threshold $S_0(T)$ was found to follow closely the T-dependence of the gluon condensate. The mass of η_c and χ_c was found to be approximately constant with respect to temperature. The width $\Gamma(T)$ first increase to a maximum at $T = 0.75T_c$ for χ_c and $T = 0.9T_c$ for η_c then decrease. The coupling constant $f(T)$ first slightly decreases then starts increasing.

The decrease in $\Gamma(T)$ and increase in $f(T)$ near the deconfinement temperature T_c suggests that the (pseudo)scalar charmonium will survive beyond T_c, and this is in agreement with lattice QCD results [22].

A paper for this project has been published in [23].

4 Light-Quark Axial-Vector Meson in Finite Temperature QCD

4.1 Finite Energy Sum Rules (FESR)

Since the Cauchy integral theorem is true for holomorphic functions, the quark hadron duality is therefore still valid if we multiply a factor of s^{N-1} $(N = 1, 2, 3...)$ to (2.7). Rewriting (2.7) with the QCD term separated into the perturbative and non-perturbative parts we have

$$4\pi^2 \int_0^R ds s^{N-1} \frac{1}{\pi} \text{Im}\Pi(s)|_{HAD} = 4\pi^2 \int_0^R ds s^{N-1} \frac{1}{\pi} \text{Im}\Pi(s)|_{PQCD} + \int_0^R ds s^{N-1} \frac{1}{\pi} \text{Im} \left[\sum_{k=1} \frac{C_2}{(-s)^k} \langle O_{2k} \rangle \right] \tag{4.1.1}$$

(The factor of $4\pi^2$ and $\frac{1}{\pi}$ is there for normalization of the integrals). From using Cauchy's theorem on the contour shown in figure 2.3 we have

$$\int_0^R ds f(s) \text{Im}\Pi(s) = -\frac{1}{2i} \oint_{|s|=R} ds f(s) \Pi(s),$$

so the second term on the right hand side of (4.1.1) becomes

$$\begin{aligned} \int_0^R ds s^{N-1} \frac{1}{\pi} \text{Im} \left[\sum_{k=1} \frac{C_{2k}}{(-s)^k} \langle O_{2k} \rangle \right] &= -\frac{1}{2\pi i} \oint ds s^{N-1} \sum_{k=1} \frac{C_{2k}}{(-s)^k} \langle O_{2k} \rangle \\ &= \frac{1}{2\pi i} \sum_{k=1} (-1)^{k-1} C_{2k} \langle O_{2k} \rangle \oint \frac{ds}{s^{k-N+1}}. \end{aligned}$$

Using the method of residues to integrate the contour integral on the right, the only non-zero term is when $k = N$, this gives

$$\begin{aligned} \frac{1}{2\pi i} \sum_{k=1} (-1)^{k-1} C_{2k} \langle O_{2k} \rangle \oint \frac{ds}{s^{k-N+1}} &= \frac{1}{2\pi i} (-1)^{N-1} C_{2N} \langle O_{2N} \rangle (2\pi i) \\ &= (-1)^{N-1} C_{2N} \langle O_{2N} \rangle. \end{aligned} \tag{4.1.2}$$

Substituting this into (4.1.1) and rearranging gives us the FESR

$$(-)^{N-1} C_{2N} \langle O_{2N} \rangle = 4\pi^2 \int_0^{S_0} ds s^{N-1} \frac{1}{\pi} \text{Im}\Pi(s)|_{HAD} - 4\pi^2 \int_0^{S_0} ds s^{N-1} \frac{1}{\pi} \text{Im}\Pi(s)|_{PQCD}. \tag{4.1.3}$$

The advantage of using this kernel is that only one condensate term is present in each sum rule equation and we do not need to choose a kernel that suppresses the excited hadronic states because the ground-state mesons dominates the spectral function in the light quark case.

4.2 Axial-Vector Current Correlator in the Chiral Limit

The correlator at zero temperature in the time-like region is given by

$$\Pi^A_{\mu\nu}(q^2) = i\int d^4x e^{iq\cdot x}\langle 0|T\left(A_\mu(x)A^\dagger_\nu(0)\right)|0\rangle \tag{4.2.1}$$

with the current $A_\mu(x)$ defined as $A_\mu(x) = \bar{d}(x)\gamma_\mu\gamma_5 u(x)$.

Evaluating the imaginary part of (4.2.1) via a similar procedure as in Section 3.2 but in the chiral limit ($m_Q = 0$) gives

$$\mathrm{Im}\Pi^A_{\mu\nu}(q^2) = \frac{1}{4\pi}\left(q_\mu q_\nu - g_{\mu\nu}q^2\right), \tag{4.2.2}$$

and for finite temperature we get

$$\mathrm{Im}\Pi^A_a(\omega^2,T) = \frac{1}{4\pi}\left[1 - 2n_F\left(\frac{\omega}{2}\right)\right] \qquad q^2 > 0 \tag{4.2.3}$$

$$\mathrm{Im}\Pi^A_s(\omega^2,T) = \frac{4}{\pi}\delta(\omega^2)\int_0^\infty y n_F(y)dy \qquad q^2 < 0. \tag{4.2.4}$$

4.3 Hadronic Terms

In the hadronic sector the correlator involves the pion pole followed by the $a_1(1260)$ resonance

$$\mathrm{Im}\Pi(s,T)|_{HAD} = \mathrm{Im}\Pi(s,T)|_\pi + \mathrm{Im}\Pi(s,T)|_{a_1}. \tag{4.3.1}$$

(If only the pion pole is used in the analysis we would obtain a $S_0 \approx 0.7\mathrm{GeV}^2$. We included the $a_1(1260)$ resonance in the analysis as we could obtain a more realistic $S_0 = 1.15\mathrm{GeV}^2$ at one-loop order and $S_0 = 1.44\mathrm{GeV}^2$ at five-loop order.)

As the pion has a very small width and mass we shall assume that the correlator is just a delta function situated at $s = 0$, ie.

$$\mathrm{Im}\Pi(s)|_\pi = 2\pi f_\pi^2(T)\delta(s) \tag{4.3.2}$$

where $f_\pi^2(0) = 92.21 \pm 0.14\mathrm{MeV}$ is the pion decay constant.

The pion decay constant is related to the quark condensate through the Gell-Mann-Oakes-Renner relation

$$2f_\pi^2 M_\pi^2 = -(m_u + m_d)\langle 0|\bar{u}u + \bar{d}d|0\rangle. \tag{4.3.3}$$

Chiral corrections to this relation are at the 5% level [24]. If we assume at finite temperature that the pion and quark masses are constants then from (4.3.3) we arrive at the relationship

$$\frac{f_\pi^2(T)}{f_\pi^2(0)} = \frac{\langle\bar{q}q\rangle(T)}{\langle\bar{q}q\rangle(0)} \tag{4.3.4}$$

($\langle\bar{q}q\rangle$ has been used as a short hand for the quark condensate). $\langle\bar{q}q\rangle(T)$ in the chiral limit has been determined using the Dyson-Schwinger equations in [26] and for finite quark masses using lattice QCD in [27]. These are shown in figure 4.1, we have used $T_c = 197MeV$ as was used in [27].

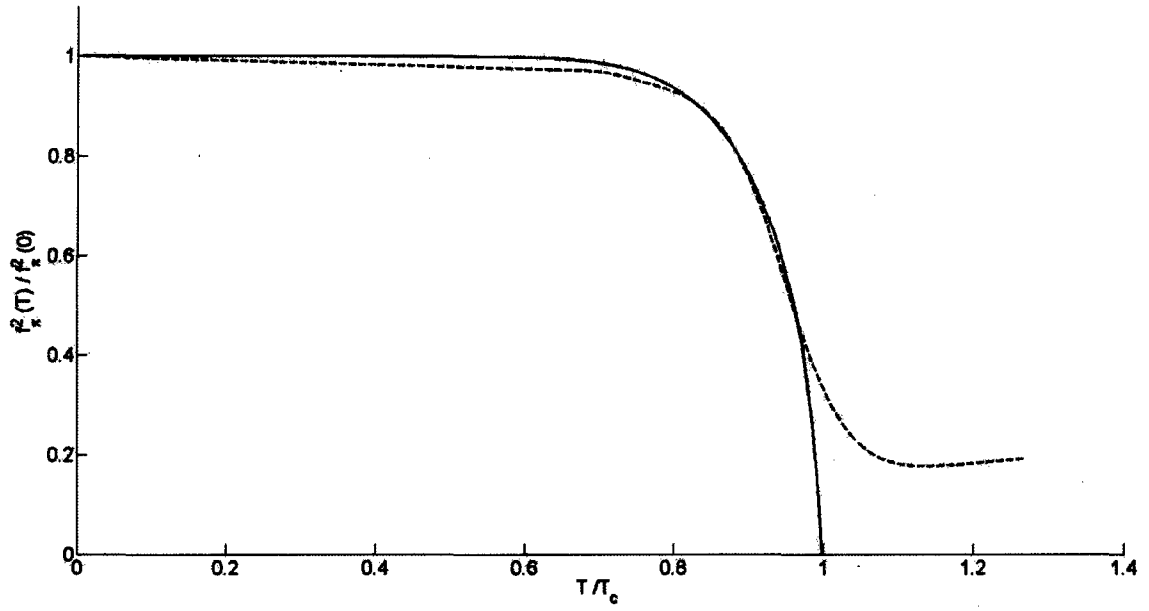

Figure 4.1: $\frac{f_\pi^2(T)}{f_\pi^2(0)}$ as a a function of T/T_c in the chiral limit ($m_q = M_\pi = 0$) (solid curve) and for finite quark masses (dotted curve) with $T_c = 197MeV$

Deviations in the Gell-Mann-Oakes-Renner relation at finite temperature is negligible except very close to the critical temperature [25].

$\mathrm{Im}\Pi(s,T)|_{a_1}$ is obtained by fitting a gaussian to the ALEPH data [28] up to $s = 1.2\mathrm{GeV}^2$ and after which $\mathrm{Im}\Pi(s,T)|_{a_1}$ was just assumed to be a constant until $s = 1.5\mathrm{GeV}^2$. Data beyond $s = 1.5\mathrm{GeV}^2$ has not been considered as in our analysis $S_0(0)$ was determined to be only $1.15\mathrm{GeV}^2$ at one-loop order and $1.44\mathrm{GeV}^2$ at five-loop order.

$$\frac{1}{\pi}\mathrm{Im}\Pi(s,T)|_{a_1} = f_{a_1}(T)C\exp\left[-\left(\frac{s-M^2}{\Gamma^2(T)}\right)^2\right] \tag{4.3.5}$$

The fit is shown in figure 4.2, and the fitting parameters are $M = 1.08906\mathrm{GeV}$, $\Gamma(0) = 0.568782\mathrm{GeV}$ and $f_{a_1}(0)C = 0.048327$. (Note: M and Γ was not labelled with the subscript a_1 because they are not the actual mass and width of the a_1, they are only fitting parameters with similar properties as the mass and width fitted to half the a_1 resonance peak). The mass will be assumed to be constant in the analysis as in the case of the heavy quarks in section 3.

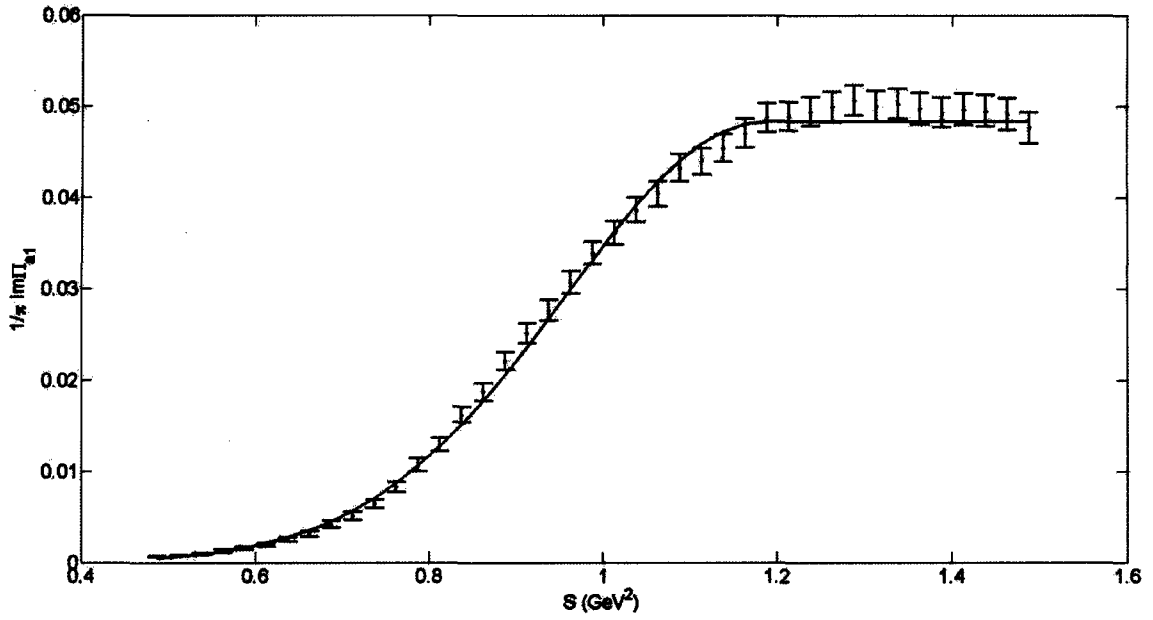

Figure 4.2: Fit to the ALEPH data in the axial-vector channel

4.4 Method

In this analysis we want to determine the behaviour of $S_0(T)$, $f_{a_1}(T)$ and $\Gamma(T)$. Since there are three unknowns we have to use the first three sum rules ie. (4.1.3) for $N = 1, 2, 3$ to determine them:

$$C_2\langle O_2\rangle = 8\pi^2 f_\pi^2(T) + 4\pi^2 \int_0^{S_0(T)} \frac{1}{\pi}\mathrm{Im}\Pi(s,T)|_{a_1} ds - 4\pi^2 \int_0^{S_0(T)} \left[\frac{1}{\pi}\mathrm{Im}\Pi_a^A(s,T) + \frac{1}{\pi}\mathrm{Im}\Pi_s^A(s,T)\right] ds$$

$$-C_4\langle O_4\rangle(T) = 4\pi^2 \int_0^{S_0(T)} s\frac{1}{\pi}\mathrm{Im}\Pi(s,T)|_{a_1} ds - 4\pi^2 \int_0^{S_0(T)} s\frac{1}{\pi}\mathrm{Im}\Pi_a^A(s,T) ds$$

$$C_6\langle O_6\rangle(T) = 4\pi^2 \int_0^{S_0(T)} s^2\frac{1}{\pi}\mathrm{Im}\Pi(s,T)|_{a_1} ds - 4\pi^2 \int_0^{S_0(T)} s^2\frac{1}{\pi}\mathrm{Im}\Pi_a^A(s,T) ds. \tag{4.4.1}$$

$C_2\langle O_2\rangle$ as stated in section 2.1 is zero. $C_4\langle O_4\rangle$ is given in (2.3) but since the quark mass here is negligible so only the gluon condensate contributes. We shall use a smoothed out version of (3.4.3) as our input for $C_4\langle O_4\rangle(T)$, this is done because the region around the kink in (3.4.3) turned out causing instabilities. The smoothed curve is shown in figure 4.3 along with lattice data from [15][29].

The leading power correction of the $C_6\langle O_6\rangle$ is the four-quark condensate, for this we shall use the vacuum saturation approximation [10]

$$C_6\langle O_6\rangle = \frac{704}{81}\pi^3\alpha_s\langle\bar{q}q\rangle^2. \tag{4.4.2}$$

One needs to note that there is no solid theoretical justification for this approximation other than the simplicity. From comparisons between (4.4.2) and direct determinations from data [12] there is in fact a

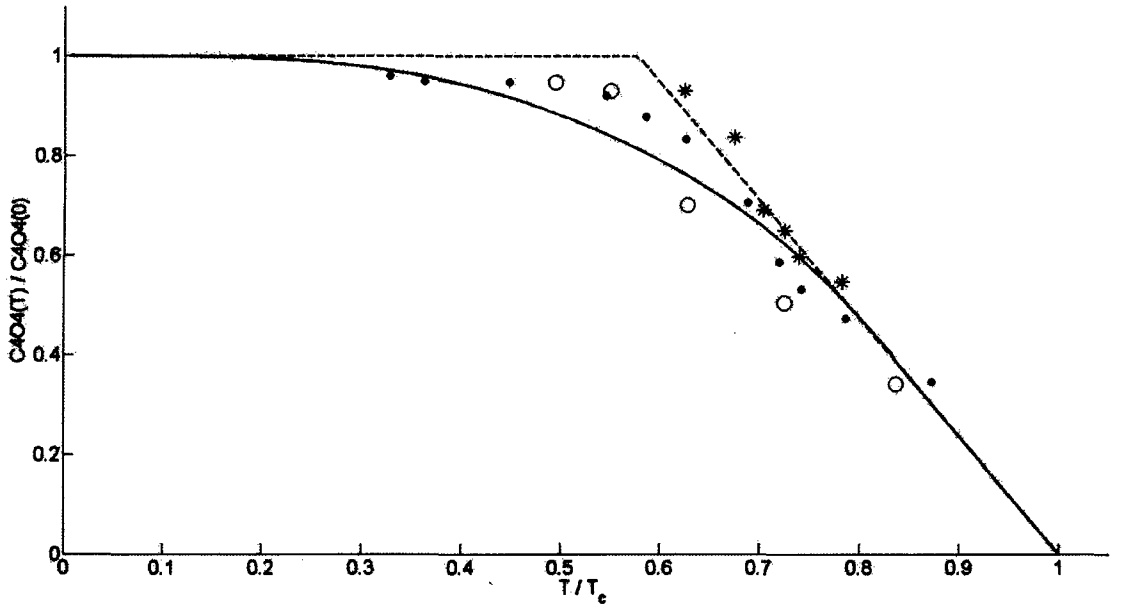

Figure 4.3: The gluon condensate $C_4\langle\hat{O}_4\rangle(T)/C_4\langle\hat{O}_4\rangle(0)$ as a function of T/T_c plotted with lattice data. Stars and circles corresponds to 2 and 4 quark flavours respectively from [15], dots corresponds to results from [29]. The dotted curve is from (3.4.3) and the solid curve is (3.4.3) but with edge smoothed out

rather large correction involved. This however should not pose a problem for us as at finite temperatures we are only interested in the behaviour of the normalized ratios of the parameters instead of their actual values.

As the three free parameters are all coupled together one has to use the Newton's Method for multi-dimensions to solve for them simultaneously.

The method works similar to the one-dimension Newton's Method but with some modifications:

$$\mathbf{x}_{\text{new}} = \mathbf{x} - \mathbf{J}^{-1}\mathbf{f}(\mathbf{x}) \tag{4.4.3}$$

where $\mathbf{x} = [S_0(T), f_{a_1}(T), \Gamma(T)]$ are the free parameters to be determined, $\mathbf{f}(\mathbf{x}) = [f_1(\mathbf{x}), f_2(\mathbf{x}), f_3(\mathbf{x})]$ are the three equations used and $\mathbf{J}$ is the Jacobian matrix $J_{ij} = df_i/dx_j$.

4.5 Zero Temperature Five-Loop Calculations

At zero temperature (4.3.5) is simply

$$\frac{1}{\pi}\text{Im}\Pi_{a_1}(s,0) = f_{a_1}(0)C\exp\left[-\left(\frac{s-M_{a_1}^2}{\Gamma^2(0)}\right)^2\right]. \tag{4.5.1}$$

Using the Weinberg Sum Rule

$$f_\rho M_\rho^2 - f_{a_1}M_{a_1}^2 = f_\pi^2 \tag{4.5.2}$$

as a rough estimate, we get $f_{a_1} = 0.073$ (using $f_\rho = 0.2$, $f_\pi = 0.092\text{GeV}$, $M_{a_1} = 1.23\text{GeV}$ and $M_\rho = 0.770\text{GeV}$). This implies $C = 0.662$.

We want to first determine S_0, $C_4\langle O_4\rangle$ and $C_6\langle O_6\rangle$ at zero temperature to see whether this value of f_{a_1} will give reasonable results. For this we use the Fixed Order Perturbation Theory (FOPT).

In FOPT the sum rule is the same as in (4.1.3) and at $T = 0$ this is

$$\begin{aligned}(-)^{N-1}C_{2N}\langle O_{2N}\rangle &= 4\pi^2\int_0^{S_0} ds s^{N-1}\frac{1}{\pi}\text{Im}\Pi(s)|_{HAD} - 4\pi^2\int_0^{S_0} ds s^{N-1}\frac{1}{\pi}\text{Im}\Pi(s)|_{PQCD} \\ &= 4\pi^2\int_0^{S_0} ds s^{N-1}\frac{1}{\pi}\text{Im}\Pi(s)|_{HAD} - \frac{S_0^N}{N}I_N(S_0). \end{aligned} \tag{4.5.3}$$

I_N determined to the five-loop order is

$$\begin{aligned}I_N(s_0) =& 1 + a_s(S_0) + [a_s(S_0)]^2\left[F_3 - \frac{\beta_1}{2}\frac{1}{N}\right] + [a_s(S_0)]^3\left[F_4 - \frac{1}{N}\left(F_3\beta_1 + \frac{\beta_2}{2}\right) + \frac{\beta_1^2}{2}\frac{1}{N^2}\right] \\ &+ [a_s(S_0)]^4\left\{k_3 - \frac{\pi^2}{4}\beta_1^2F_3 - \frac{5}{24}\pi^2\beta_1\beta_2 - \frac{1}{N}\left[\frac{3}{2}\beta_1\left(F_4 + \frac{\pi^2}{3}\frac{\beta_1^2}{4}\right) + \beta_2F_3 + \frac{\beta_3}{2} - \frac{\pi^2}{8}\beta_1^3\right]\right. \\ &\left. + \frac{2}{N^2}\frac{\beta_1}{2}\left(\frac{3}{2}\beta_1F_3 + \frac{5}{4}\beta_2\right) - \frac{6}{N^3}\frac{\beta_1^3}{8}\right\} \end{aligned} \tag{4.5.4}$$

where $\beta_1 = -9/2$, $\beta_2 = -67/6$, $\beta_3 = -3863/192$,$k_3 = 25$, $F_3 = 1.6398$ and $F_4 = -10.2839$. The strong coupling constant, $a_s(S_0) \equiv \frac{\alpha_s(S_0)}{\pi}$, to five-loop order is

$$\begin{aligned}\frac{\alpha_s^{(3)}(S_0)}{\pi} =& \frac{\alpha_s^{(1)}(S_0)}{\pi} + \left(\frac{\alpha_s^{(1)}(S_0)}{\pi}\right)^2\left(\frac{-\beta_2}{\beta_1}\ln L\right) + \left(\frac{\alpha_s^{(1)}(S_0)}{\pi}\right)^3\left(\frac{\beta_2^2}{\beta_1^2}(\ln^2 L - \ln L - 1) + \frac{\beta_3}{\beta_1}\right) \\ &- \left(\frac{\alpha_s^{(1)}(S_0)}{\pi}\right)^4\left[\frac{\beta_2^3}{\beta_1^3}\left(\ln^3 L - \frac{5}{2}\ln^2 L - 2\ln L + \frac{1}{2}\right) + 3\frac{\beta_2\beta_3}{\beta_1^2}\ln L + \frac{b_3}{\beta_1}\right] \end{aligned} \tag{4.5.5}$$

where $\frac{\alpha_s^{(1)}(S_0)}{\pi} = \frac{-2}{\beta_1 L}$, $L = \ln(S_0/\Lambda^2)$ and

$$b_3 = \frac{1}{4^4}\left[\frac{149753}{6} + 3564\zeta_3 - \left(\frac{1078361}{162} + \frac{6508}{27}\zeta_3\right)n_F + \left(\frac{50065}{162} + \frac{6472}{81}\zeta_3\right)n_F^2 + \frac{1093}{729}n_F^3\right] \tag{4.5.6}$$

with $\zeta_3 = 1.202$ and $n_F = 3$.

For $\Lambda = 350\text{MeV}$ it is determined from the first three sum rules that $S_0 = 1.44\text{GeV}^2$, $C_4\langle O_4\rangle = -0.024\text{GeV}^4$ and $C_6\langle O_6\rangle = 0.301\text{GeV}^6$. This result agrees with that found in [12].

4.6 Finite Temperature Results

To give the correct value of $f_{a_1}(0) = 0.073$ at the one-loop order it was determined that $C_6\langle O_6\rangle(0) = -0.037\text{GeV}^6$ and $C_4\langle O_4\rangle(0) = 0.191\text{GeV}^4$.

At one-loop order $S_0(0)$ is determined to be 1.15GeV^2, it decreases to around $0.62S_0(0)$ at $0.83T_c$ beyond which the method gives no more solutions. If we extrapolate the result we see that S_0 should reach zero around $0.9T_c$. Result for $S_0(T)$ with the extrapolation is shown in Figure 4.4.

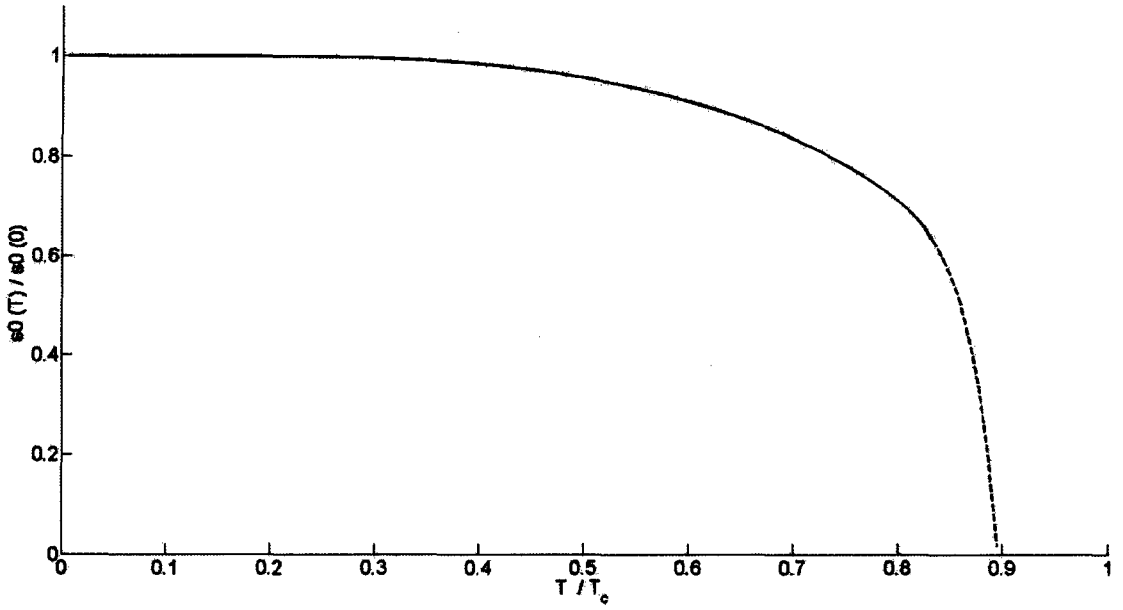

Figure 4.4: $S_0(T)/S_0(0)$ against T/T_c, dotted line is an extrapolation of the result

Result for $f_{a_1}(T)/f_{a_1}(0)$ is shown in Figure 4.5. It first starts increasing until it come to a maximum at $0.72T_c$ after which it decreases. Extrapolating the result shows that it would reach zero around $0.9T_c$ as well.

$\Gamma(T)/\Gamma(0)$ is shown in Figure 4.6 and is seen to be monotonically increasing.

The results obtained when using the quark condensate of finite quark masses (dotted curve in figure 4.1) is very similar to that in chiral limit case since the method give no more solutions after $0.83T_c$ so it will not be affected by the finite mass quark condensate flattening as this happens only after T_c.

4.7 Conclusion

From the FESR we have determined the behaviour of the continuum threshold $S_0(T)$, the coupling of the $a_1(1260)$ to the axial-vector current, $f_{a_1}(T)$, and a parameter with characteristics of the $a_1(1260)$ width, $\Gamma(T)$. By assuming the $a_1(1260)$ mass to be temperature independent and the pion pole not broaden with temperature, it was found that $S_0(T)$ and $f_{a_1}(T)$ decreases with temperature and would reach zero around $0.9T_c$. $\Gamma(T)$ was found to be monotonically increasing. The increase of $\Gamma(T)$ and the decrease of $f_{a_1}(T)$ are indicative of a transition to a quark-gluon deconfined phase at $T \approx T_c$. This also provides additional support for the interpretation of $S_0(T)$ as a phenomenological order parameter for quark-gluon deconfinement.

A paper for this project has been published in [30].

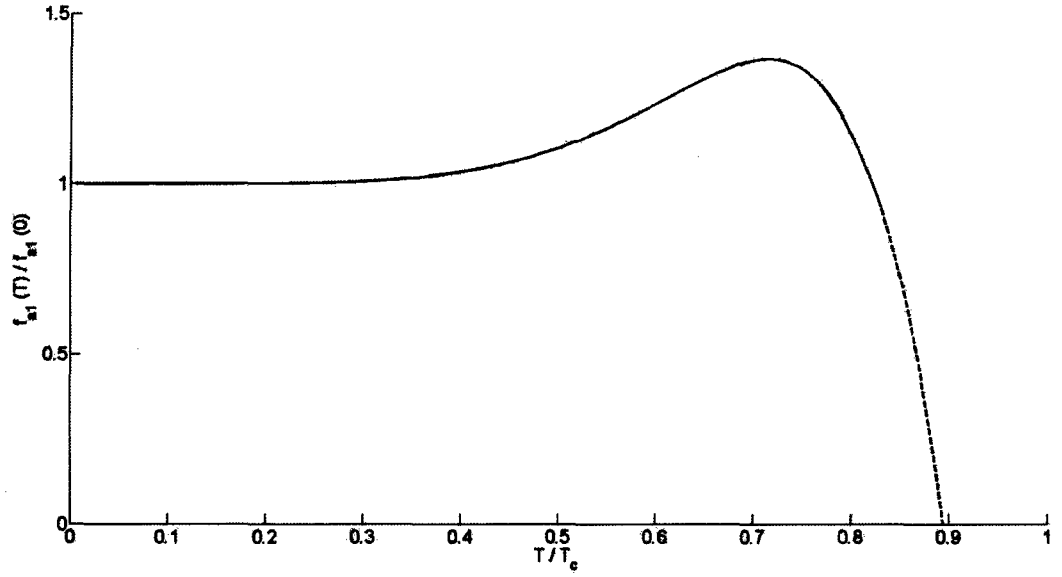

Figure 4.5: $f_{a_1}(T)/f_{a_1}(0)$ against T/T_c, dotted line is an extrapolation of the result

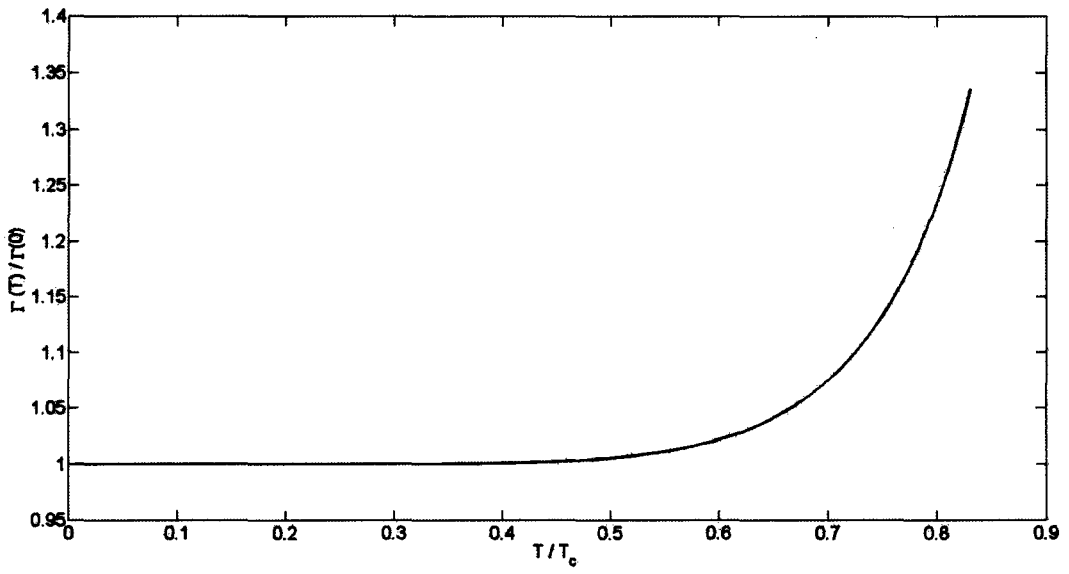

Figure 4.6: $\Gamma(T)/\Gamma(0)$ against T/T_c

5 Light-Quark Vector Meson in Finite Temperature QCD

5.1 FESR

For the vector mesons we shall use the same FESR as in section 4 but with a normalization factor of $8\pi^2$ instead of $4\pi^2$. This is due to an extra factor of $1/2$ in the $\mathrm{Im}\Pi(s)|_{PQCD}$ term.

$$(-)^{N-1}C_{2N}\langle O_{2N}\rangle = 8\pi^2\int_0^{S_0} ds s^{N-1}\frac{1}{\pi}\mathrm{Im}\Pi(s)|_{HAD} - 8\pi^2\int_0^{S_0} ds s^{N-1}\frac{1}{\pi}\mathrm{Im}\Pi(s)|_{PQCD}. \tag{5.1.1}$$

5.2 Vector Current Correlator in the Chiral Limit

The vector current correlator at zero temperature in the time-like region is given by

$$\Pi^V_{\mu\nu}(q^2) = i\int d^4x e^{iq\cdot x}\langle 0|T\left(V_\mu(x)V^\dagger_\nu(0)\right)|0\rangle \tag{5.2.1}$$

where the current $V_\mu(x)$ is $V_\mu(x) = \frac{1}{2}\left[\bar{d}(x)\gamma_\mu d(x) - \bar{u}(x)\gamma_\mu u(x)\right]$.

In the chiral limit the imaginary part of (5.2.1) is evaluated to be

$$\mathrm{Im}\Pi^V_{\mu\nu}(q^2) = \frac{1}{8\pi}\left(q_\mu q_\nu - g_{\mu\nu}q^2\right). \tag{5.2.2}$$

For finite temperature we get

$$\mathrm{Im}\Pi^V_a(\omega^2,T) = \frac{1}{8\pi}\left[1 - 2n_F\left(\frac{\omega}{2}\right)\right] \qquad q^2 > 0 \tag{5.2.3}$$

$$\mathrm{Im}\Pi^V_s(\omega^2,T) = \frac{2}{\pi}\delta(\omega^2)\int_0^\infty y n_F(y)dy \qquad q^2 < 0. \tag{5.2.4}$$

5.3 Hadronic Terms

We shall assume that the correlator in the hadronic sector is saturated by only the ρ-meson.

The ρ-meson resonance will be approximated by a Breit-Wigner and is given by

$$\frac{1}{\pi}\mathrm{Im}\Pi(s)|_{HAD} = \frac{1}{\pi}\frac{1}{f_\rho^2}\frac{M_\rho^3\Gamma_\rho}{\left(S - M_\rho^2\right)^2 + M_\rho^2\Gamma_\rho^2} \tag{5.3.1}$$

where $f_\rho = 5$, $M_\rho = 0.776\mathrm{GeV}$ and $\Gamma_\rho = 0.145\mathrm{GeV}$.

There is also a space-like region contribution to the hadronic sector due to the coupling of ρ-meson to two pions in the thermal bath, this was determined to be

$$\frac{1}{\pi}\text{Im}\Pi(\omega,T)|^s_{HAD} = \frac{2}{3\pi^2}\delta(\omega^2)\int_0^\infty y n_B(y)dy. \tag{5.3.2}$$

where $n_B(Z) = (e^{Z/T}-1)^{-1}$ is the Bose thermal function.

5.4 Zero Temperature Five-Loops Calculation

We use the FOPT as in section 4.5 to determine values for S_0, $C_4\langle\hat{O}_4\rangle$ and $C_6\langle\hat{O}_6\rangle$ at zero temperature for checking whether our method will give reasonable results.

The sum rule is

$$(-)^{N-1}C_{2N}\langle\hat{O}_{2N}\rangle = 8\pi^2\int_0^{S_0} ds s^{N-1}\frac{1}{\pi}\text{Im}\Pi(s)|_{HAD} - \frac{S_0^N}{N}I_N(S_0), \tag{5.4.1}$$

where I_N determined to the five-loop order is given in (4.5.4).

For $\Lambda = 350$MeV it is determined from the first three sum rules with $C_2\langle\hat{O}_2\rangle = 0$ that $S_0 = 1.44\text{GeV}^2$, $C_4\langle\hat{O}_4\rangle = 0.12\text{GeV}^4$ and $C_6\langle\hat{O}_6\rangle = -0.39\text{GeV}^6$. This result agrees with that found in [12]

5.5 Method

In the analysis of the ρ-meson we use a similar approach as we did for the $a_1(1260)$ where we shall use the first three sum rules of (5.1.1). However we have found that in the case of the ρ the results are very sensitive to the behaviour of the input parameters.

Using the approximation (4.4.2) for $C_6\langle\hat{O}_6\rangle(T)$ and a constant ρ mass as input parameters is no longer able to generate reasonable results (decreasing $S_0(T)$ and $f_\rho(T)$, and increasing $\Gamma_\rho(T)$). Using the lattice results for $C_4\langle\hat{O}_4\rangle(T)$ is also not possible as there is no data at low temperatures, and low temperature behaviours is found to affect the final ρ results greatly.

After much trial and error it was found that results which agrees with expectations for $S_0(T)$, $f_\rho(T)$ and $C_4\langle\hat{O}_4\rangle(T)$ could be obtained by using the following anstaz for $\Gamma_\rho(T)$, $C_6\langle\hat{O}_6\rangle(T)$ and $M_\rho(T)$ as input parameters

$$\Gamma_\rho(T) = \frac{\Gamma_\rho(0)}{1-(T/T_c)^a} \tag{5.5.1}$$

where $T_c = 197$MeV (chosen to be the same as that in the axial-vector channel), $a = 3 \pm 1$

$$C_6\langle\hat{O}_6\rangle(T) = C_6\langle\hat{O}_6\rangle(0)(1-(T/T_q^*)^b \tag{5.5.2}$$

where at one loop order $C_6\langle\hat{O}_6\rangle(0) = -0.952\text{GeV}^6$, $T_q^* = 187 \pm 3$MeV, $b = 8 \pm 4$

$$M_\rho(T) = M_\rho(T)(1-(T/T_m^*)^c) \tag{5.5.3}$$

where $T_m^* = 222 \pm 10$MeV, $c = 10 \pm 3$ (these parameters for $M_\rho(T)$ are deliberately chosen so that $M_\rho(T)$ only decreases slightly at T_c).

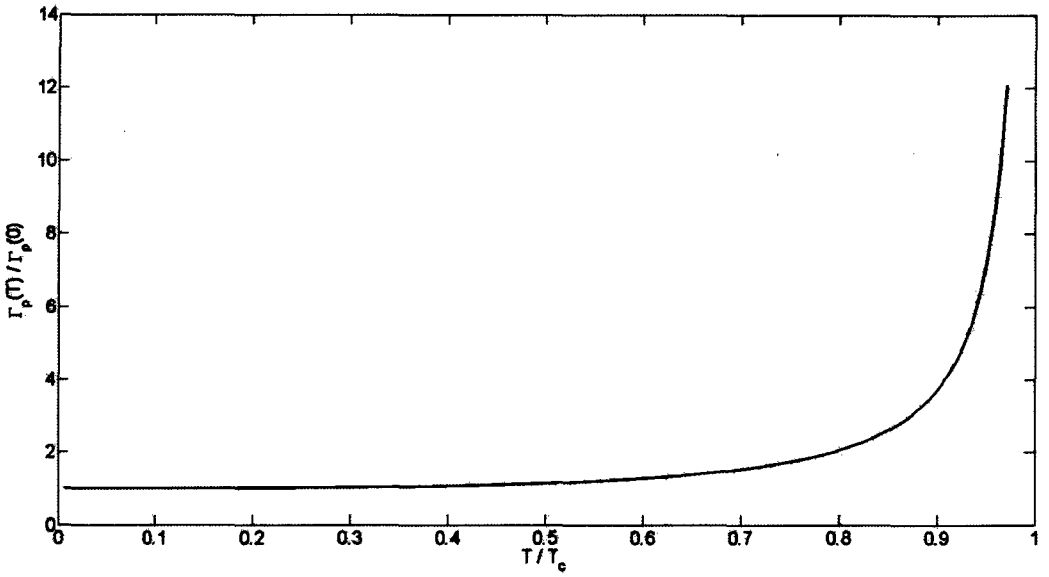

Figure 5.1: $\Gamma_\rho(T)/\Gamma_\rho(0)$ against T/T_c using (5.5.1) with $a = 3$

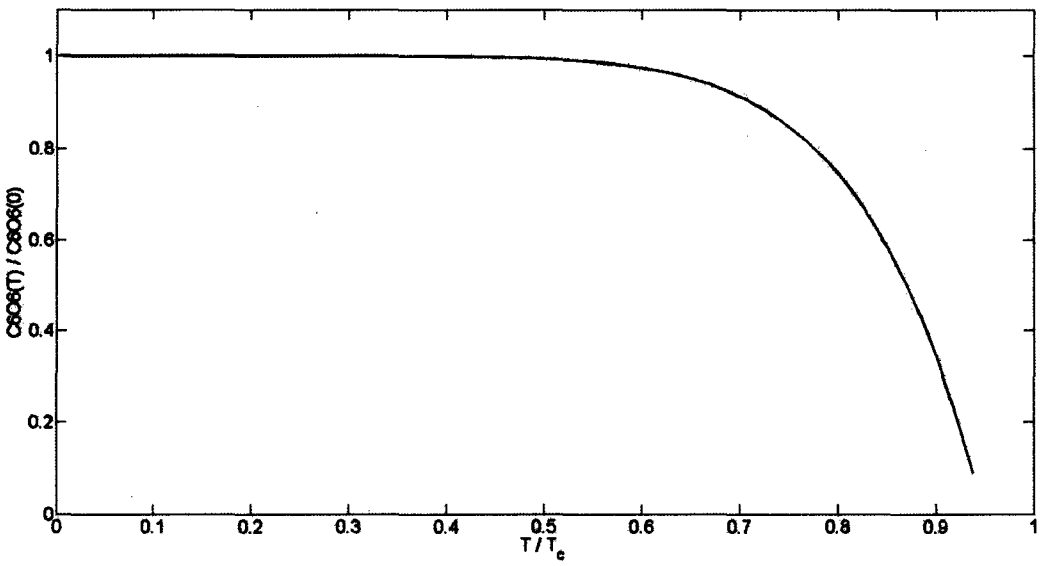

Figure 5.2: $C_6\langle\hat{O}_6\rangle(T)/C_6\langle\hat{O}_6\rangle(0)$ against T/T_c using (5.5.2) with $T_q^* = 187\text{MeV}$ and $b = 8$

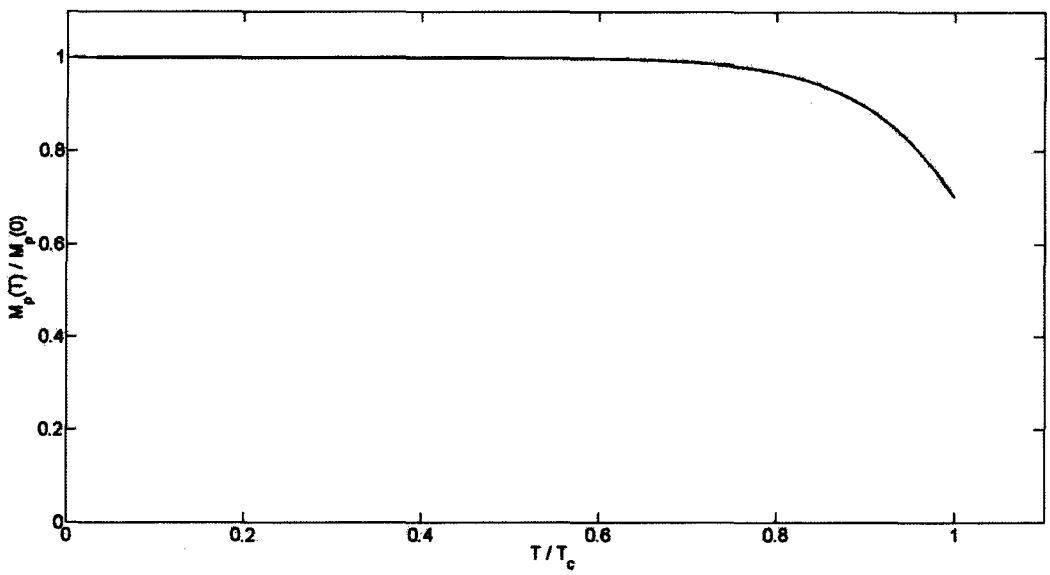

Figure 5.3: $M_\rho(T)/M_\rho(0)$ against T/T_c using (5.5.3) with $T_m* = 222\text{MeV}$ and $c = 10$

5.6 Results and Conclusions

Result for $S_0(T)$ is shown in Figure 5.4 and is seen to decrease with temperature. A solution can only be found until $0.94T_c$, after extrapolating the curve it can be seen that $S_0(T)$ should reach zero at $0.98T_c$. At one loop order $S_0(0) = 1.73\text{GeV}^2$. A fit to the results gives $S_0(T)/S_0(0) = 1 - 0.5667(T/T_c)^{11.38} - 4.347(T/T_c)^{68.41}$

$f_\rho(T)$ is shown in Figure 5.5. $f_\rho(T)$ first increases slightly and then starts decreasing at around $0.7T_c$. After extrapolating the curve beyond $0.94T_c$ it can be seen that $f_\rho(T)$ should reach zero at $1.1T_c$. A fit to the results gives $f_\rho(T)/f_\rho(0) = 1 - 0.3901(T/T_c)^{10.75} + 0.04155(T/T_c)^{1.269}$.

$C_4\langle\hat{O}_4\rangle(T)$ is shown in Figure 5.6 together with a rescaled lattice result from [29], the two have a very good agreement. $C_4\langle\hat{O}_4\rangle(T)$ is found to first increase slightly then decrease to zero at $T = T_q^*$. A fit to the results gives $C_4\langle\hat{O}_4\rangle(T)/C_4\langle\hat{O}_4\rangle(0) = 1 - 1.65(T/T_c)^{8.735} + 0.04967(T/T_c)^{0.7211}$.

All results agrees with expectations that for a disappearing ρ-meson $S_0(T)$ and $f_\rho(T)$ will decrease while $\Gamma_\rho(T)$ increases with temperature while both $C_4\langle\hat{O}_4\rangle(T)$ and $C_6\langle\hat{O}_6\rangle(T)$ disappears at T_c.

A paper for this project has been submitted to Physical Review D and has just been accepted for publication [31].

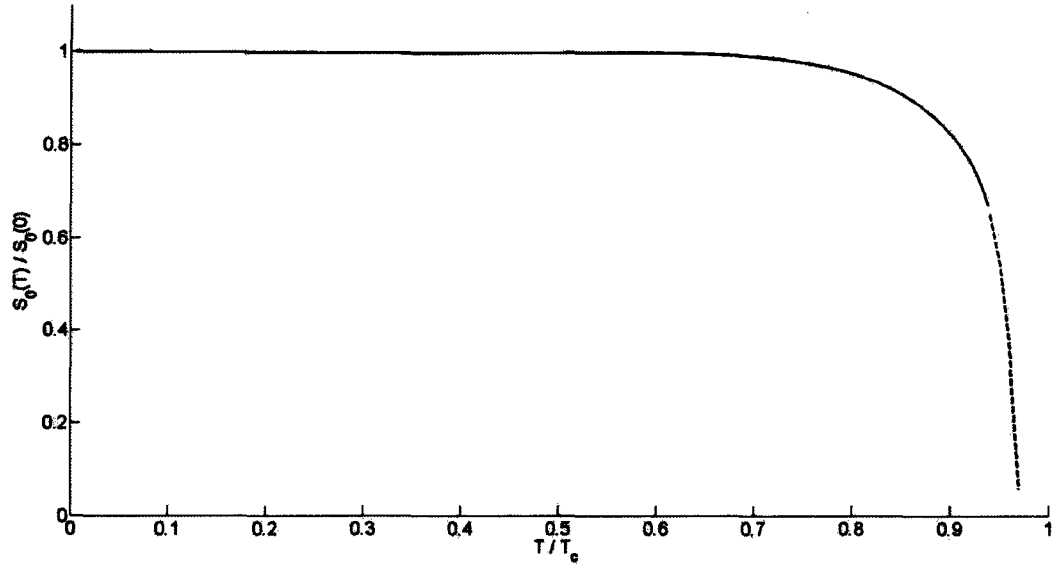

Figure 5.4: $S_0(T)/S_0(0)$ against T/T_c, dotted line is an extrapolation of the result

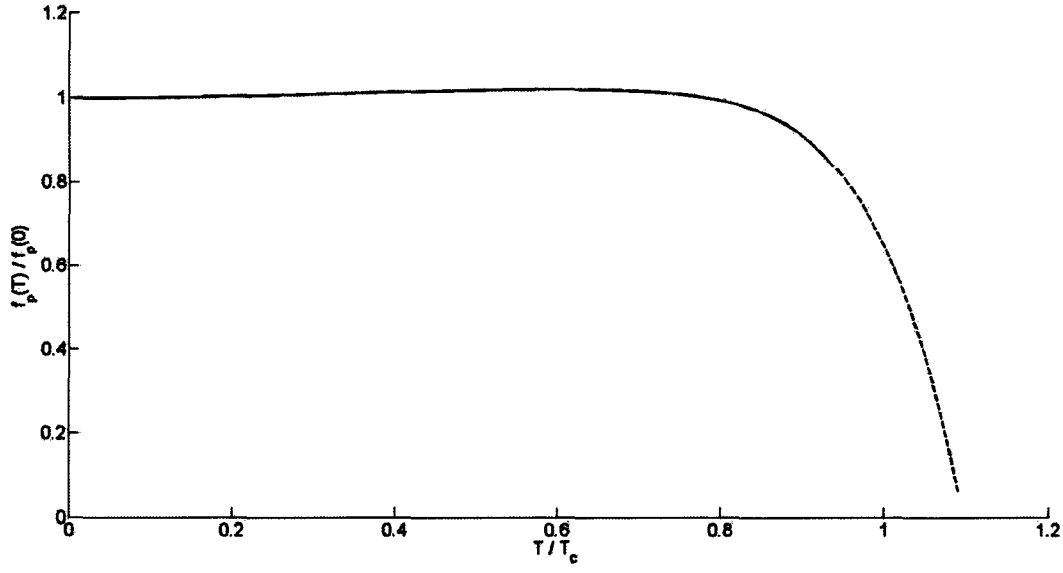

Figure 5.5: $f_\rho(T)/f_\rho(0)$ against T/T_c, dotted line is an extrapolation of the result

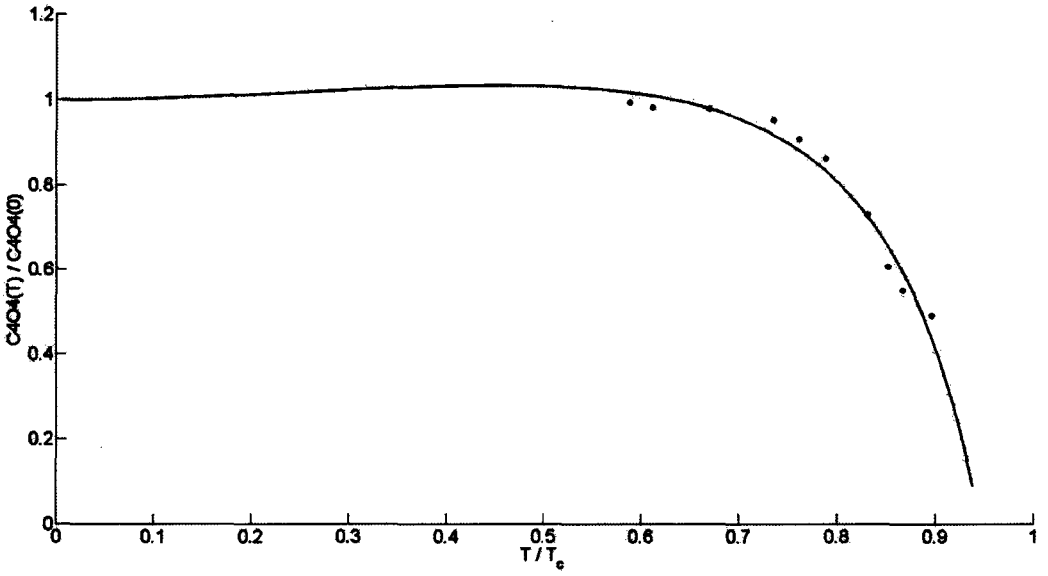

Figure 5.6: $C_4\langle\hat{O}_4\rangle(T)/C_4\langle\hat{O}_4\rangle(0)$ against T/T_c, dots corresponds to lattice results from [29]

6 Light-Quark Axial-Vector Meson in Finite Density QCD

6.1 Finite Energy Sum Rules (FESR)

The FESR is the same as that in section 4 and is given by

$$(-)^{N-1}C_{2N}\langle O_{2N}\rangle = 4\pi^2\int_0^{S_0} ds s^{N-1}\frac{1}{\pi}\mathrm{Im}\Pi(s)|_{HAD} - 4\pi^2\int_0^{S_0} ds s^{N-1}\frac{1}{\pi}\mathrm{Im}\Pi(s)|_{PQCD}. \tag{6.1.1}$$

6.2 Correlator in the Time Like Region for Axial Vector Particles in Chiral Limit

At finite temperature and density the virtual quanta with time like momenta $q^2 > 0$ are converted into quark-antiquark pairs at a rate proportional to $[1-n_+(k_0)][1-n_-(k_0-q_0)]$ or $[1-n_-(k_0)][1-n_+(k_0-q_0)]$. At the same time quanta are produced in the matter at a rate proportional to $n_+(k_0)n_-(k_0-q_0)$ or $n_-(k_0)n_+(k_0-q_0)$ where $n_\pm(x) = \left(e^{(x\mp\mu)/T}+1\right)^{-1}$ are the Fermi-Dirac thermal distributions for particles and antiparticles.

The correlator is then given by

$$\begin{aligned}\Pi_{\mu\nu}(q^2)|_a^A &= \frac{i}{2}\int d^4x e^{iq\cdot x}\langle 0|T\left(A_\mu(x)A_\mu^\dagger(x)\right)|0\rangle\{[1-n_+(k_0)][1-n_-(k_0-q_0)] - n_+(k_0)n_-(k_0-q_0)\\ &+ [1-n_-(k_0)][1-n_+(k_0-q_0)] - n_-(k_0)n_+(k_0-q_0)\}\\ &= \frac{i}{2}\int d^4x e^{iq\cdot x}\langle 0|T\left(A_\mu(x)A_\mu^\dagger(x)\right)|0\rangle[2-n_+(k_0)-n_-(k_0-q_0)-n_-(k_0)-n_+(k_0-q_0)].\end{aligned} \tag{6.2.1}$$

Evaluating (6.2.1) in the chiral limit as done in previous sections gives

$$\mathrm{Im}\Pi_a^A(q^2,T,\mu) = \frac{1}{4\pi}\left[1-n_+\left(\frac{\omega}{2}\right)-n_-\left(\frac{\omega}{2}\right)\right]. \tag{6.2.2}$$

6.3 Correlator in the Space Like Region for Axial Vector Particles in Chiral Limit

In the space like region where quanta has momenta $q^2 < 0$, quanta may be absorbed by the quarks and antiquarks in the medium at a rate of $n_+(k_0)[1-n_-(k_0-q_0)]$ or $n_-(k_0)[1-n_+(k_0-q_0)]$ and then re-emitted at a rate of $n_+(k_0-q_0)[1-n_-(k_0)]$ or $n_-(k_0-q_0)[1-n_+(k_0)]$. The correlator in the space like

region is then

$$\begin{aligned}\Pi_{\mu\nu}(q^2)|_s^A &= \frac{i}{2}\int d^4x e^{iq\cdot x}\langle 0|T\left(A_\mu(x)A_\mu^\dagger(x)\right)|0\rangle \{n_+(k_0)\left[1-n_-(k_0-q_0)\right]-n_+(k_0-q_0)\left[1-n_-(k_0)\right] \\ &+ n_-(k_0)\left[1-n_+(k_0-q_0)\right]-n_-(k_0-q_0)\left[1-n_+(k_0)\right]\} \\ &= \frac{i}{2}\int d^4x e^{iq\cdot x}\langle 0|T\left(A_\mu(x)A_\mu^\dagger(x)\right)|0\rangle \left[\Delta n_+(k_0)+\Delta n_-(k_0)\right]. \end{aligned} \tag{6.3.1}$$

where $\Delta n_\pm(k_0) \equiv n_\pm(k_0) - n_\pm(k_0 - q_0)$.

Evluating (6.3.1) gives

$$\begin{aligned}\mathrm{Im}\Pi_s^A(q^2,T,\mu) &= \frac{2}{\pi}\delta(\omega^2)\left[\int_0^\infty y\left[n_+(y)+n_-(y)\right]dy\right] \\ &= \frac{1}{\pi}\delta(\omega^2)\left(\mu^2+\frac{\pi^2T^2}{3}\right)\end{aligned} \tag{6.3.2}$$

6.4 Quark Condensate

For the quark condensate at finite temperature and density we use the expression derived in [9],

$$\langle\overline{\psi}\psi\rangle(T,\mu) = \langle\overline{\psi}\psi\rangle|_0 - \frac{8TN_c}{\pi^2}\sum_{l=1}^{\infty}\frac{(-1)^l}{l}\cosh\left(\frac{l\mu}{T}\right)\sum_{i=4}^{4}\frac{r_i m_i^2}{|b_i|^3}K_1\left(\frac{l|m_i|}{T}\right), \tag{6.4.1}$$

where $\langle\overline{\psi}\psi\rangle|_0 = -(0.241\mathrm{GeV})^3$ is the quark condensate at zero T and μ, $K_1(x)$ is a bessel function. Values of b_i, m_i and r_i for $i = 1,2,3$ are given in the table below and b_4, m_4 and r_4 are variables that must be determined by fitting to data.

i	b_i	m_i(GeV)	r_i
1	1	-0.490	-0.112
2	1	0.495	0.352
3	1	-0.879	0.259

First a polynomial was fitted to the lattice data [27] and the following expression was obtained

$$\langle\overline{\psi}\psi\rangle_{\mathrm{fit}} = \begin{cases} \frac{11.623-112.2T+274.8T^2}{8330.5T-87362.5T^2+233983.2T^3} & T > 140\mathrm{MeV} \\ -0.00299399T+0.013997 & T \le 140\mathrm{MeV} \end{cases} \tag{6.4.2}$$

This was done so (6.4.1) could be fitted to data with a finer grid of temperature.

(6.4.1) was then fitted to (6.4.2), since there are two variables , $\frac{r_4}{|b_4|^3}$ and m_4, yet only one equation so we let $m_4 = 0.4$GeV and $\frac{r_4}{|b_4|^3}$ been chosen to be the fitting parameter. The fitted result for $\frac{r_4}{|b_4|^3}$ is shown in Fig.6.1.

In Figure 6.2, (6.4.1) is plotted against T at various μ using the obtained values of $\frac{r_4}{|b_4|^3}$. We can see that (6.4.1) is not valid for $T < 0.7$GeV because $\langle\overline{\psi}\psi\rangle$ becomes greater than zero for small values of μ ($\mu < 100$ MeV), this cannot be possible.

From Figure 6.3 in which I plotted (6.4.1) against μ for various T's, we can see that for $T < 140$MeV the density μ_c at which $\langle\overline{\psi}\psi\rangle$ reaches zero increases with respect to T and for $T > 140$MeV μ_c decreases with T. (6.4.1) is not valid for $\mu > 0.4$GeV as the summation starts to diverge.

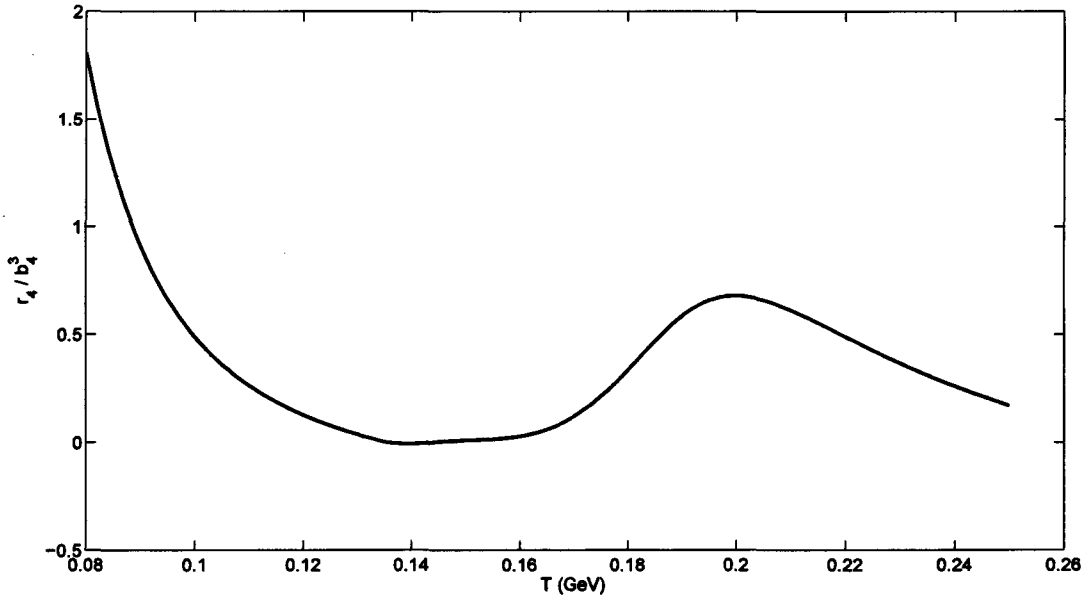

Figure 6.1: $\frac{r_4}{|b_4|^3}$ against T with $m_4 = 0.4\text{GeV}$.

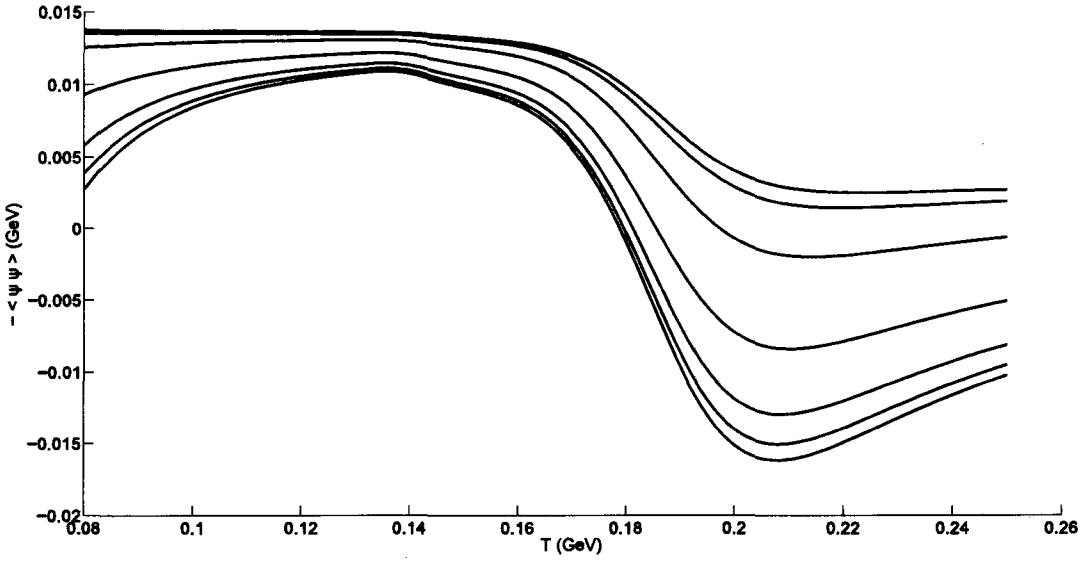

Figure 6.2: $-\langle\overline{\psi}\psi\rangle$ against T at different μ. From the top curve to the bottom curve $\mu = 0$, 100, 200, 300, 350, 370, 380 MeV respectively

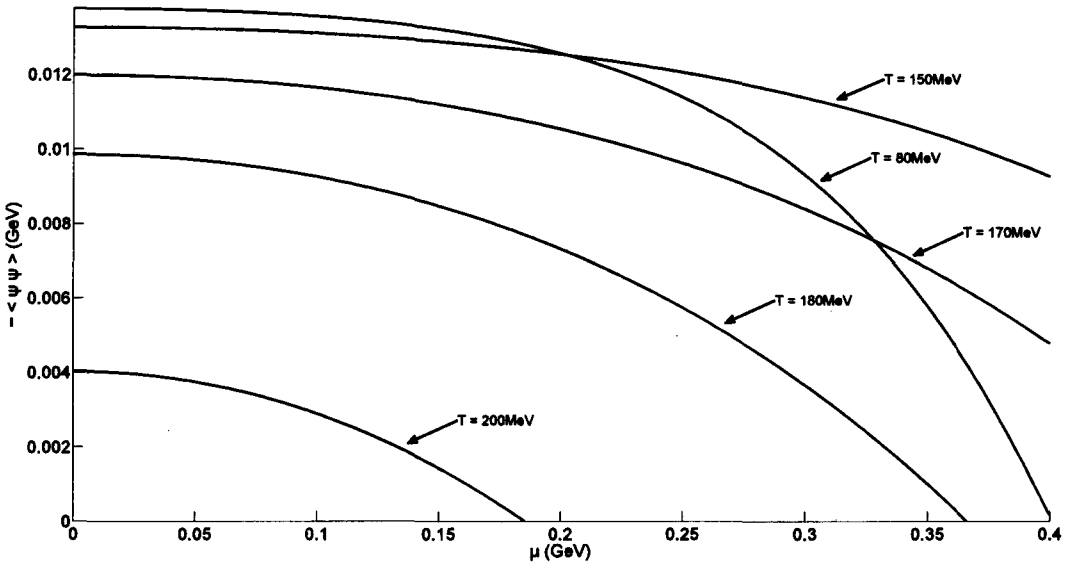

Figure 6.3: $-\langle\bar{\psi}\psi\rangle$ against μ for different T

6.5 Hadronic Term

We use the same hadronic terms as that in section 4 i.e. the pion pole followed by the $a_1(1260)$ resonance

$$\frac{1}{\pi}\text{Im}\Pi(s,T,\mu)|_{HAD} = 2\pi f_\pi^2(T,\mu)\delta(s) + f_{a_1}(T,\mu)C\exp\left[-\left(\frac{s-M^2}{\Gamma^2(T,\mu)}\right)^2\right] \tag{6.5.1}$$

where $f_\pi^2(0) = 92.21 \pm 0.14\text{MeV}$, $M = 1.08906\text{GeV}$, $\Gamma(0) = 0.568782\text{GeV}$ and $f_{a_1}(0)C = 0.048327$.

From the Gell-Mann-Oakes-Renner relation (4.3.3) we get an expression for $\frac{f_\pi^2(T,\mu)}{f_\pi^2(0)}$

$$\frac{f_\pi^2(T,\mu)}{f_\pi^2(0)} = \frac{\langle\bar{\psi}\psi\rangle(T,\mu)}{\langle\bar{\psi}\psi\rangle(0)}. \tag{6.5.2}$$

6.6 Method

For this analysis one cannot choose T to be too small as (6.4.1) is not valid at small temperatures as seen in Figure 6.2. One also could not choose T between 80 and 170 MeV as μ_c, which is required for the behaviour of $\Gamma(\mu)$, cannot be determined in this range of temperatures (see Figure 6.3). For $T > 170\text{MeV}$ there is no solution for S_0 as shown from the results at finite temperature in section 4. Lucky there is still a small window of temperatures $T \approx 80\text{MeV}$ in which we can explore finite density behaviours.

From (6.1.1) we have three sum rules at our disposal

$$C_2\langle O_2\rangle = 8\pi^2 f_\pi^2(T,\mu) + 4\pi^2 \int_0^{S_0(T,\mu)} \frac{1}{\pi}\mathrm{Im}\Pi(s,T,\mu)|_{a_1} ds - 4\pi^2 \int_0^{S_0(T,\mu)} \left[\frac{1}{\pi}\mathrm{Im}\Pi_a^A(s,T,\mu) + \frac{1}{\pi}\mathrm{Im}\Pi_s^A(s,T,\mu)\right] ds$$

$$-C_4\langle O_4\rangle(T,\mu) = 4\pi^2 \int_0^{S_0(T,\mu)} s\frac{1}{\pi}\mathrm{Im}\Pi(s,T,\mu)|_{a_1} ds - 4\pi^2 \int_0^{S_0(T,\mu)} s\frac{1}{\pi}\mathrm{Im}\Pi_a^A(s,T,\mu) ds$$

$$C_6\langle O_6\rangle(T,\mu) = 4\pi^2 \int_0^{S_0(T,\mu)} s^2\frac{1}{\pi}\mathrm{Im}\Pi(s,T,\mu)|_{a_1} ds - 4\pi^2 \int_0^{S_0(T,\mu)} s^2\frac{1}{\pi}\mathrm{Im}\Pi_a^A(s,T,\mu) ds. \tag{6.6.1}$$

$C_2\langle O_2\rangle$ as before will be assumed to be zero and for $C_6\langle \hat{O}_6\rangle$ we use the approximation given in (4.4.2)

$$C_6\langle O_6\rangle(T,\mu) = \frac{704}{81}\pi^3\alpha_s\langle\overline{\psi}\psi\rangle^2(T,\mu). \tag{6.6.2}$$

There is no lattice data for $C_4\langle O_4\rangle$ at finite density so we shall treat it as a parameter to be determined. This leaves us with four unknown parameters $S_0(T,\mu)$, $f_{a_1}(T,\mu)$, $\Gamma(T,\mu)$ and $C_4\langle O_4\rangle(T,\mu)$ yet only three equations. We will need to make some approximation on one of the parameters and use it as input, for this we chose $\Gamma(T,\mu)$.

We use a slightly modified anstaz for $\Gamma(T,\mu)$ to that given in (5.5.1) so μ dependence can be included

$$\Gamma(T,\mu) = \frac{\Gamma(0)}{1 - \left(\frac{T}{T_c}\right)^\alpha - \left(\frac{\mu}{\mu_c}\right)^\beta} \tag{6.6.3}$$

To obtain similar results at finite temperature as in section 4. α is chosen to be 8 and to obtain the correct behaviour of $S_0(\mu)$ (monotonically decreasing), β has to be 3.

6.7 Results and Conclusion

Result for $S_0(\mu)$ is shown in Figure 6.4. $S_0(\mu=0)$ is determined to be $1.10\mathrm{GeV}^2$ at $T = 80\mathrm{MeV}$, it steadily decreases to about $0.72S_0(\mu=0)$ at $0.69\mu_c$ beyond which there is no more solutions.

Result for $f_{A_1}(\mu)$ is shown in Figure 6.5. It first starts increasing until it come to a maximum at $0.3\mu_c$ after which it decreases.

Result for $C_4\langle\hat{O}_4\rangle(\mu)$ is shown in Figure 6.6. $C_4\langle\hat{O}_4\rangle(\mu=0)$ is determined to be $0.174\mathrm{GeV}^4$ at $T = 80\mathrm{MeV}$ and steadily decrease with μ. $C_4\langle\hat{O}_4\rangle(\mu)$ cannot be determined beyond $0.69T_c$ as that is the limit to which $S_0(\mu)$ can be determined. However an extension of the end point of $C_4\langle\hat{O}_4\rangle(\mu)$ by a straight line shows that it should reach zero at $\approx 0.85\mu_c$.

These results agrees with the expectation that if the hadron disappears at μ_c, $S_0(\mu)$, $f_{a_1}(\mu)$ and $C_4\langle O_4\rangle(\mu)$ will decrease and $\Gamma(\mu)$ will increase with density. Expanding the analysis to a larger range of temperatures requires a more accurate expression for $\langle\overline{\psi}\psi\rangle$ to be developed which is beyond the scope of this project.

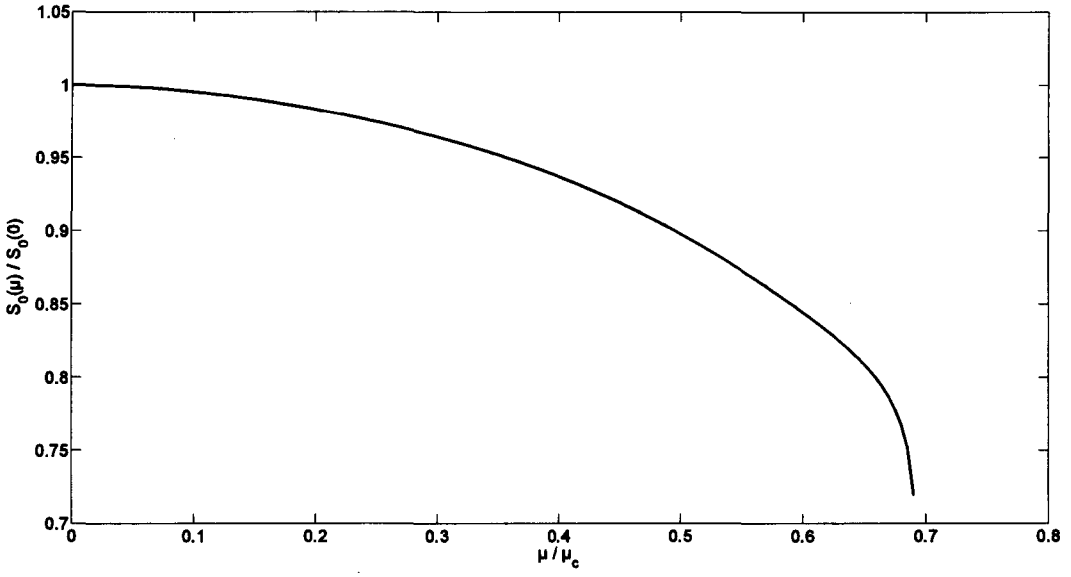

Figure 6.4: $\frac{S_0(\mu)}{S_0(0)}$ against $\frac{\mu}{\mu_c}$ at $T = 80\text{MeV}$

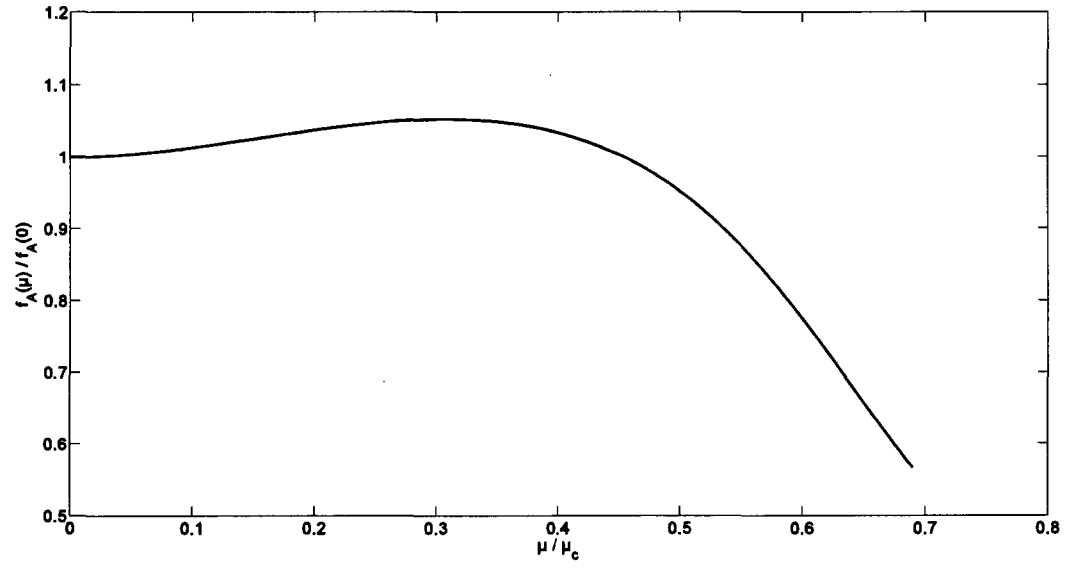

Figure 6.5: $\frac{f_{A1}(\mu)}{f_{A1}(0)}$ against $\frac{\mu}{\mu_c}$ at $T = 80\text{MeV}$

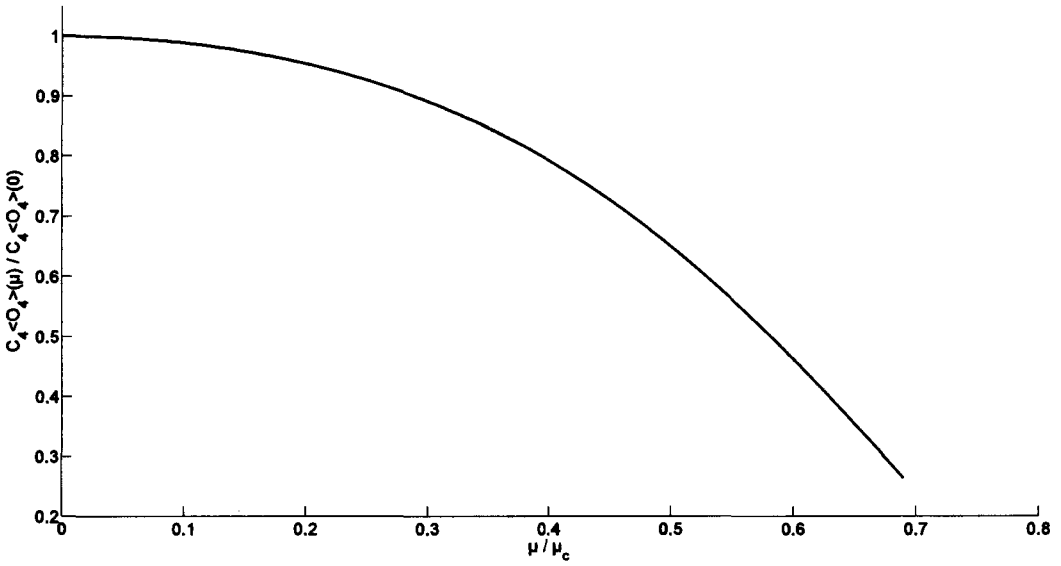

Figure 6.6: $\frac{C_4\langle\hat{O}_4\rangle(\mu)}{C_4\langle\hat{O}_4\rangle(0)}$ against $\frac{\mu}{\mu_c}$ at $T = 80\text{MeV}$

A Computing the Imaginary Part of $f(k^2) = \frac{1}{k^2-m^2}$

Define

$$\begin{aligned} \mathrm{Disc} f(k^2) &\equiv f(k^2 + i\epsilon) - f(k^2 - i\epsilon) \\ &= \frac{1}{k^2 - m^2 + i\epsilon} - \frac{1}{k^2 - m^2 - i\epsilon} \\ &= \frac{-2i\epsilon}{(k^2 - m^2)^2 + \epsilon^2} \end{aligned}$$

Looking at figure A.1 we see that

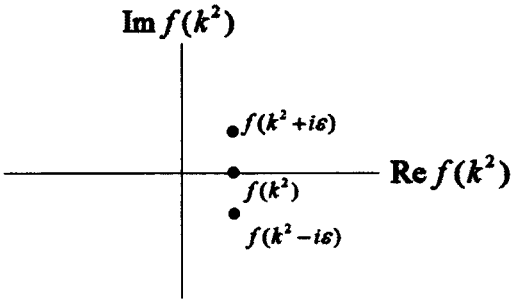

Figure A.1:

$$\begin{aligned} \mathrm{Im} f(k^2) &= \epsilon \overset{lim}{\to} 0 \, \frac{1}{2i} \mathrm{Disc} f(k^2) \\ &= \frac{-\epsilon}{(k^2 - m^2)^2 + \epsilon^2} \end{aligned} \tag{A.1}$$

and since

$$\int_{-\infty}^{\infty} \frac{dk^2}{(k^2 - m^2)^2 + \epsilon^2} = \frac{1}{\epsilon} \tan^{-1} \frac{k^2 - m^2}{\epsilon} \Bigg|_{-\infty}^{\infty} = \frac{\pi}{\epsilon}$$

$$\Rightarrow \frac{1}{(k^2 - m^2)^2 + \epsilon^2} = \frac{\pi}{\epsilon} \delta(k^2 - m^2)$$

therefore

$$\begin{aligned}
\mathrm{Im}f(k^2) &= -\pi\delta(k^2-m^2) \\
&= -\frac{\pi}{2|k_0|}\left[\delta\left(k_0-\sqrt{|\vec{k}|^2+m_Q^2}\right)+\delta\left(k_0+\sqrt{|\vec{k}|^2+m_Q^2}\right)\right] \\
&= -\pi\left[\delta(k^2-m^2)\Theta(k_0)+\delta(k^2-m^2)\Theta(-k_0)\right] \\
&\equiv -\pi\left[\delta^{(+)}(k^2-m_Q^2)+\delta^{(-)}(k^2-m_Q^2)\right] \qquad \text{(A.2)}
\end{aligned}$$

where

$$\Theta(z)\equiv\begin{cases}0 & z<0\\ 1 & z>0\end{cases}$$

Note: For the case of $\delta[(k-q)^2-m_Q^2]$ we have

$$\delta^{(+)}[(k-q)^2-m_Q^2]=\delta[(k-q)^2-m_Q^2]\begin{cases}\Theta(k_0-q_0)\\ \text{or}\\ \Theta(q_0-k_0)\end{cases} \qquad \text{(A.3)}$$

We will see in Appendix B that in the limit $|\vec{q}|\to 0$, when $q^2>0$

$$k_0=\sqrt{|\vec{k}|^2+m_Q^2}\approx 1/2q_0<q_0$$

$$\Rightarrow \delta^{(+)}[(k-q)^2-m_Q^2]=\delta[(k-q)^2-m_Q^2]\Theta(q_0-k_0) \quad \text{for} \quad q^2>0,$$

and when $q^2<0$, $|\vec{k}|$ will have no upper bound yet q_0 becomes 0 therefore

$$k_0=\sqrt{|\vec{k}|^2+m_Q^2}>q_0$$

$$\Rightarrow \delta^{(+)}[(k-q)^2-m_Q^2]=\delta[(k-q)^2-m_Q^2]\Theta(k_0-q_0) \quad \text{for} \quad q^2<0.$$

B Thermal Phase Space Integrals in the Limit $|\vec{q}| \to 0$ in the Time-Like Region $q^2 > 4m_Q^2$

In this section we would attempt to work out the following thermal phase space integrals

$$
\begin{aligned}
(I_1)_{\mu\nu} &= \int d^4k \delta^{(+)}\left[k^2 - m_Q^2\right] \delta^{(+)}\left[(k-q)^2 - m_Q^2\right] \left[n_F\left(|k_0|\right) + n_F\left(|k_0 - q_0|\right)\right] k_\mu k_\nu \\
I_2 &= \int d^4k \delta^{(+)}\left[k^2 - m_Q^2\right] \delta^{(+)}\left[(k-q)^2 - m_Q^2\right] \left[n_F\left(|k_0|\right) + n_F\left(|k_0 - q_0|\right)\right] k^2 \\
(I_3)_{\mu\nu} &= \int d^4k \delta^{(+)}\left[k^2 - m_Q^2\right] \delta^{(+)}\left[(k-q)^2 - m_Q^2\right] \left[n_F\left(|k_0|\right) + n_F\left(|k_0 - q_0|\right)\right] q_\mu k_\nu \\
I_4 &= \int d^4k \delta^{(+)}\left[k^2 - m_Q^2\right] \delta^{(+)}\left[(k-q)^2 - m_Q^2\right] \left[n_F\left(|k_0|\right) + n_F\left(|k_0 - q_0|\right)\right] q \cdot k
\end{aligned}
\tag{B.1}
$$

in the time-like region $q^2 > 4m_Q^2$ and in the limit $|\vec{q}| \to 0$.

The solution to $(I_1)_{\mu\nu}$ would have the form of $\left(Aq_\mu q_\nu + Bg_{\mu\nu}q^2\right) I_1$ where A and B are constants, therefore

$$
\left(Aq_\mu q_\nu + Bg_{\mu\nu}q^2\right) I_1 = \int d^4k \delta^{(+)}\left[k^2 - m_Q^2\right] \delta^{(+)}\left[(k-q)^2 - m_Q^2\right] \left[n_F\left(|k_0|\right) + n_F\left(|k_0 - q_0|\right)\right] k_\mu k_\nu. \tag{B.2}
$$

Multiplying (B.2) by $q^\mu q^\nu$ we get

$$
(A+B)q^4 I_1 = \int d^4k \delta^{(+)}\left[k^2 - m_Q^2\right] \delta^{(+)}\left[(k-q)^2 - m_Q^2\right] \left[n_F\left(|k_0|\right) + n_F\left(|k_0 - q_0|\right)\right] (k \cdot q)^2, \tag{B.3}
$$

and multiplying (B.2) by $g^{\mu\nu}$ we get

$$
(A+4B)q^2 I_1 = \int d^4k \delta^{(+)}\left[k^2 - m_Q^2\right] \delta^{(+)}\left[(k-q)^2 - m_Q^2\right] \left[n_F\left(|k_0|\right) + n_F\left(|k_0 - q_0|\right)\right] k^2. \tag{B.4}
$$

We will begin by solving (B.3) first (Θ functions will be omitted). We first rewrite (B.3) as

$$
\begin{aligned}
(A+B)I_1 = \frac{1}{q^4} \int d^4k \frac{1}{2k_0} \delta\left[k_0 - \sqrt{|\vec{k}|^2 + m_Q^2}\right] \delta\left[k_0^2 - |\vec{k}|^2 - 2k_0 q_0 + 2|\vec{k}||\vec{q}|\cos\theta + q^2 - m_Q^2\right] \\
\times \left[n_F\left(|k_0|\right) + n_F\left(|k_0 - q_0|\right)\right] \left(k_0 q_0 - |\vec{k}||\vec{q}|\cos\theta\right)^2,
\end{aligned}
\tag{B.5}
$$

integrate with respect to k_0

$$(A+B)I_1 = \frac{1}{2q^4}\int d^3k \frac{1}{\sqrt{|\vec{k}|^2+m_Q^2}}\delta\left[q^2 - 2\sqrt{|\vec{k}|^2+m_Q^2}q_0 + 2|\vec{k}||\vec{q}|\cos\theta\right]\left(\sqrt{|\vec{k}|^2+m_Q^2}q_0 - |\vec{k}||\vec{q}|\cos\theta\right)^2$$
$$\times\left[n_F\left(\left|\sqrt{|\vec{k}|^2+m_Q^2}\right|\right) + n_F\left(\left|\sqrt{|\vec{k}|^2+m_Q^2} - q_0\right|\right)\right], \tag{B.6}$$

rewrite in spherical polar coordinates and rename the parameters as

$$u \equiv |\vec{k}|, \quad \omega \equiv q_0, \quad z \equiv \cos\theta, \quad z^* \equiv \frac{1}{2|\vec{q}|u}\left(-q^2 + 2\omega\sqrt{u^2+m_Q^2}\right)$$

we obtain

$$(A+B)I_1 = \frac{\pi}{q^4}\int_{u_1}^{u_2}\frac{u^2du}{\sqrt{u^2+m_Q^2}}\int_{-1}^{1}\frac{dz}{2u|\vec{q}|}\delta(z-z^*)\left[u|\vec{q}|\left(\frac{\omega\sqrt{u^2+m_Q^2}}{u|\vec{q}|} - z\right)\right]^2$$
$$\times\left[n_F\left(\left|\sqrt{u^2+m_Q^2}\right|\right) + n_F\left(\left|\sqrt{u^2+m_Q^2} - \omega\right|\right)\right], \tag{B.7}$$

finally integrating with respect to z we get

$$(A+B)I_1 = \frac{\pi}{q^4}\int_{u_1}^{u_2}\frac{u^2du}{\sqrt{u^2+m_Q^2}}\frac{1}{2u|\vec{q}|}\left[u|\vec{q}|\left(\frac{\omega\sqrt{u^2+m_Q^2}}{u|\vec{q}|} - z^*\right)\right]^2\left[n_F\left(\left|\sqrt{u^2+m_Q^2}\right|\right) + n_F\left(\left|\sqrt{u^2+m_Q^2} - \omega\right|\right)\right]$$

$$= \frac{\pi}{q^4}\frac{1}{2|\vec{q}|}\int_{u_1}^{u_2}\frac{udu}{\sqrt{u^2+m_Q^2}}\left[u|\vec{q}|\left(\frac{q^2}{2u|\vec{q}|}\right)\right]^2\left[n_F\left(\left|\sqrt{u^2+m_Q^2}\right|\right) + n_F\left(\left|\sqrt{u^2+m_Q^2} - \omega\right|\right)\right]$$

$$= \frac{\pi}{16}\frac{1}{|\vec{q}|}\int_{u_1^2}^{u_2^2}\frac{du^2}{\sqrt{u^2+m_Q^2}}\left[n_F\left(\left|\sqrt{u^2+m_Q^2}\right|\right) + n_F\left(\left|\sqrt{u^2+m_Q^2} - \omega\right|\right)\right]. \tag{B.8}$$

To determine the integration limits u_1 and u_2 we use the fact that $-1 \le z^* \le 1$ since $-1 \le z = \cos\theta \le 1$

$$\begin{cases} \frac{1}{2|\vec{q}|u_2}\left(-q^2 + 2\omega\sqrt{u_2^2+m_Q^2}\right) = 1 \\ \frac{1}{2|\vec{q}|u_1}\left(-q^2 + 2\omega\sqrt{u_1^2+m_Q^2}\right) = -1 \end{cases}$$

$$\begin{cases} 4q^2u_2^2 - 4|\vec{q}|u_2q^2 - q^4 + 4\omega^2m_Q^2 = 0 \\ 4q^2u_1^2 + 4|\vec{q}|u_1q^2 - q^4 + 4\omega^2m_Q^2 = 0 \end{cases} \tag{B.9}$$

in the limit $|\vec{q}| \to 0$, $q^2 \to \omega^2$ so (B.9) becomes

$$\begin{cases} 4\omega^2 u_2^2 - 4|\vec{q}|u_2\omega^2 - \omega^4 + 4\omega^2 m_Q^2 = 0 \\ 4\omega^2 u_1^2 + 4|\vec{q}|u_1\omega^2 - \omega^4 + 4\omega^2 m_Q^2 = 0 \end{cases}$$

$$\begin{cases} 4u_2^2 - 4|\vec{q}|u_2 - \omega^2 v^2 = 0 \\ 4u_1^2 + 4|\vec{q}|u_1 - \omega^2 v^2 = 0 \end{cases} \qquad \text{where} \quad v \equiv \sqrt{1 - 4\frac{m_Q^2}{\omega^2}}$$

$$\begin{cases} u_2 = \frac{1}{2}(|\vec{q}| \pm \omega v) + O(|\vec{q}|^2) \\ u_1 = \frac{1}{2}(-|\vec{q}| \pm \omega v) + O(|\vec{q}|^2) \end{cases} \tag{B.10}$$

As $u \geq 0$ and $\omega \geq 2m_Q > 0$ therefore only the positive root of (B.10) is valid

$$\Rightarrow \begin{cases} u_2 = \frac{1}{2}(|\vec{q}| + \omega v) \\ u_1 = \frac{1}{2}(-|\vec{q}| + \omega v) \end{cases}$$

$$\begin{cases} u_2^2 = \frac{1}{4}(2|\vec{q}|\omega v + \omega^2 v^2) + O(|\vec{q}|^2) \\ u_1^2 = \frac{1}{4}(-2|\vec{q}|\omega v + \omega^2 v^2) + O(|\vec{q}|^2) \end{cases} \tag{B.11}$$

To evaluate (B.8) we need to do a change of variables where we let

$$x^2 = \frac{4\omega^2}{|\vec{q}|^2}\left(u^2 - \frac{1}{4}\omega^2 v^2\right) = \frac{4\omega^2}{|\vec{q}|^2}\left(u^2 - \frac{\omega^2}{4} + m_Q^2\right) \tag{B.12}$$

$$\Rightarrow \begin{cases} x_2^2 = \frac{2}{|\vec{q}|}\omega^3 v \\ x_1^2 = -\frac{2}{|\vec{q}|}\omega^3 v \end{cases},$$

and (B.8) becomes

$$(A+B)I_1 = \frac{\pi}{16}\frac{1}{|\vec{q}|}\int_{x_1^2}^{x_2^2} \frac{\frac{|\vec{q}|^2}{4\omega^2}dx^2}{\sqrt{\frac{|\vec{q}|^2}{4\omega^2}x^2 + \frac{\omega^2}{4}}}\left[n_F\left(\left|\sqrt{\frac{|\vec{q}|^2}{4\omega^2}x^2 + \frac{\omega^2}{4}}\right|\right) + n_F\left(\left|\sqrt{\frac{|\vec{q}|^2}{4\omega^2}x^2 + \frac{\omega^2}{4}} - \omega\right|\right)\right]$$

$$= \frac{\pi}{16}\int_{x_1^2}^{x_2^2} \frac{\frac{|\vec{q}|}{4\omega^2}dx^2}{\frac{\omega}{2}}\left[n_F\left(\left|\frac{\omega}{2}\right|\right) + n_F\left(\left|-\frac{\omega}{2}\right|\right)\right] + O(|\vec{q}|^2)$$

$$= \frac{\pi}{16}\frac{|\vec{q}|}{\omega^3}n_F\left(\left|\frac{\omega}{2}\right|\right)\int_{x_1^2}^{x_2^2} dx^2$$

$$= \frac{\pi v}{4}n_F\left(\left|\frac{\omega}{2}\right|\right). \tag{B.13}$$

To evaluate (B.4) we follow the same procedures as above and we obtain

$$(A+4B)I_1 = \frac{\pi v m_Q^2}{\omega^2}n_F\left(\left|\frac{\omega}{2}\right|\right). \tag{B.14}$$

From the above we see that

$$I_1 = \frac{1}{A+B}\frac{\pi v}{4} n_F\left(\left|\frac{\omega}{2}\right|\right) = \frac{1}{A+4B}\frac{\pi v m_Q^2}{\omega^2} n_F\left(\left|\frac{\omega}{2}\right|\right) \tag{B.15}$$

and after rearranging we get a relationship between A and B

$$Av^2 = \frac{4}{\omega^2} B(m_Q^2 - \omega^2). \tag{B.16}$$

By choosing

$$B = -v^2 = -\frac{1}{4\omega^2}(\omega^2 - 4m_Q^2) \tag{B.17}$$

$$\Rightarrow A = \frac{1}{\omega^2}(\omega^2 - m_Q^2), \tag{B.18}$$

we get in the limit $|\vec{q}| \to 0$

$$\begin{aligned}(I_1)_{\mu\nu} &= \left(Aq_\mu q_\nu + Bg_{\mu\nu}q^2\right)\frac{1}{A+B}\frac{\pi v}{4} n_F\left(\left|\frac{\omega}{2}\right|\right) \\ &= \frac{1}{\omega^2}\left[q_\mu q_\nu\left(\omega^2 - m_Q^2\right) - \frac{1}{4}g_{\mu\nu}\omega^2\left(\omega^2 - 4m_Q^2\right)\right]\frac{\pi v}{3} n_F\left(\left|\frac{\omega}{2}\right|\right),\end{aligned} \tag{B.19}$$

and

$$I_2 = g^{\mu\nu}(I_1)_{\mu\nu} = \pi v m_q^2 n_F\left(\left|\frac{\omega}{2}\right|\right). \tag{B.20}$$

The solution to $(I_3)_{\mu\nu}$ is of the form $q_\mu q_\nu I_3$. If we multiply both sides of the equation by $g^{\mu\nu}$ we get

$$q^2 I_3 = \int d^4k \delta^{(+)}\left[k^2 - m_Q^2\right]\delta^{(+)}\left[(k-q)^2 - m_Q^2\right]\left[n_F\left(|k_0|\right) + n_F\left(|k_0 - q_0|\right)\right] q\cdot k \tag{B.21}$$

Performing a similar calculation to that of calculating (B.3) we get

$$(I_3)_{\mu\nu} = \frac{\pi v}{2} q_\mu q_\nu n_F\left(\left|\frac{\omega}{2}\right|\right), \tag{B.22}$$

and

$$I_4 = g^{\mu\nu}(I_3)_{\mu\nu} = \frac{\pi v}{2}\omega^2 n_F\left(\left|\frac{\omega}{2}\right|\right). \tag{B.23}$$

C Computing the Correlator in the Time-like Region Using Finite Temperature Propagator

The correlator of pseudoscalar particles at finite temperature is

$$\Pi_5(q^2) = i \int d^4x e^{iq\cdot x} \left\langle\left\langle \left| [J_5(x), J_5^\dagger(0)] \right| \right\rangle\right\rangle \tag{C.1}$$

with

$$\langle\langle |A \cdot B| \rangle\rangle = \sum_n \frac{e^{-E_n/T} \langle n | A \cdot B | n \rangle}{\mathrm{Tr} e^{-H/T}} \tag{C.2}$$

being the Gibbs average and $|n\rangle$ is any complete set of eigenstates of the (QCD) Hamiltonian.

It is derived in [21] that the propagator at finite temperature for fermions is

$$S_F(k)_T = \frac{\not{k} + m}{k^2 - m^2} + 2\pi i(\not{k} + m)\delta(k^2 - m^2) n_F(|k_0|) . \tag{C.3}$$

The correlator is now simply

$$\Pi_5(T) = iN_c \int d^4x \int \frac{d^4k_1}{(2\pi)^4} \int \frac{d^4k_2}{(2\pi)^4} \int d^4x e^{iq\cdot x} e^{-ik_1\cdot x} e^{ik_2\cdot x} \mathrm{Tr}\left[S_F(k_1)_T \gamma_5 S_F(k_2)_T \gamma_5\right] . \tag{C.4}$$

Integrating with respect to x and k_2 then renaming $k_1 \equiv k$ we get

$$\Pi_{\mu\nu}(T) = iN_c \int \frac{d^4k}{(2\pi)^4} \mathrm{Tr}\left[S_F(k)_T \gamma_5 S_F(k-q)_T \gamma_5\right] \tag{C.5}$$

and

$$\begin{aligned}
\mathrm{Tr}\left[S_F(k)_T\gamma_5 S_F(k-q)_T\gamma_5\right] &= \mathrm{Tr}\left\{\left[\frac{\not k+m_Q}{k^2-m_Q^2}+2\pi i(\not k+m_Q)\delta(k^2-m_Q^2)n_F\left(|k_0|\right)\right]\gamma_5\right. \\
&\left.\times\left[\frac{\not k-\not q+m_Q}{(k-q)^2-m_Q^2}+2\pi i(\not k-\not q+m_Q)\delta[(k-q)^2-m_Q^2]n_F\left(|k_0-q_0|\right)\right]\gamma_5\right\} \\
&= \mathrm{Tr}\left[-\frac{\not k+m_Q}{k^2-m_Q^2}\frac{\not k-\not q+m_Q}{(k-q)^2-m_Q^2}\gamma_5^2\right] \\
&+ 2\pi i n_F\left(|k_0-q_0|\right)\delta[(k-q)^2-m_Q^2]\mathrm{Tr}\left[-\frac{\not k+m_Q}{k^2-m_Q^2}(\not k-\not q+m_Q)\gamma_5^2\right] \\
&+ 2\pi i n_F\left(|k_0|\right)\delta(k^2-m_Q^2)\mathrm{Tr}\left[-\frac{\not k-\not q+m_Q}{(k-q)^2-m_Q^2}(\not k+m_Q)\gamma_5^2\right] \\
&+ \text{term without imaginary part} \\
&= \frac{-4(k^2-q\cdot k-m_Q^2)}{[(k-q)^2-m_Q^2][k^2-m_Q^2]}(k^2-q\cdot k-m_Q^2)-8\pi i\left[(k^2-q\cdot k-m_Q^2)\right] \\
&\times\left\{n_F\left(|k_0|\right)\frac{\delta(k^2-m_Q^2)}{(k-q)^2-m_Q^2}+n_F\left(|k_0-q_0|\right)\frac{\delta[(k-q)^2-m_Q^2]}{k^2-m_Q^2}\right\} \qquad \text{(C.6)} \\
&+ \text{term without imaginary part.}
\end{aligned}$$

The imaginary part of $\Pi_5(T)$ is then

$$\begin{aligned}
\mathrm{Im}\Pi_5(q^2,T) &= -8N_c\pi^2\int\frac{d^4k}{(2\pi)^4}\left(k^2-q\cdot k-m_Q^2\right) \\
&\times\left\{1-n_F(|k_0|)-n_F(|k_0-q_0|)\right\}\delta(k^2-m_Q^2)\delta([(k-q)^2-m_Q^2] \qquad \text{(C.7)}
\end{aligned}$$

D Relation Between Gluon Condensate and Trace of Energy Momentum Tensor

In most lattice results at finite temperature [15][29], the trace of the energy momentum tensor $\Theta^{\mu}_{\mu}(T)$ is determined instead of the gluon condensate.

From [15] the relationship between the two is given as follows

$$\left\langle \frac{\alpha_s}{\pi} G^a_{\mu\nu} G^{a\mu\nu} \right\rangle\Big|_T = \left\langle \frac{\alpha_s}{\pi} G^a_{\mu\nu} G^{a\mu\nu} \right\rangle\Big|_0 - \frac{96\pi^2}{33 - 2n_F} \Theta^{\mu}_{\mu}(T) \tag{D.1}$$

where n_F is the number of quark flavours and

$$\Theta^{\mu}_{\mu}(T) = \epsilon - 3P \tag{D.2}$$

with ϵ the energy density and P the pressure for relativistic fields and relativistic hydrodynamics.

Bibliography

[1] M.A. Shifman, A.I. Vainshtein and V.I. Zakharov, Nucl. Phys. B 147, 385 (1979); M.A. Shifman, A.I. Vainshtein and V.I. Zakharov, Nucl. Phys. B 147, 448 (1979).

[2] A.I. Bochkarev and M.E. Shaposnikov, Nucl. Phys. B 268, 220 (1986).

[3] C.A. Dominguez and M. Loewe, Phys. Rev. D 52, 3143 (1995).

[4] C.A. Dominguez and M. Loewe, Z. Phys. C , Particles & Fields 51, 69 (1991).

[5] C.A. Dominguez, M. Loewe and J.C. Rojas, JHEP 0708, 40 (2007).

[6] C.A. Dominguez and M. Loewe, Z. Phys. C , Particles & Fields 49, 423 (1991).

[7] C.A. Dominguez, M. Loewe, J.C. Rojas and Y. Zhang, Phy. Rev. D 81, 014007 (2010).

[8] A.L.S. Angelis *et al.*, HELIOS-3 Collaboration, Eur. Phys. J. C 13, 433 (2000); M.C. Abreu *et al.*, NA38/NA50 Collaboration, Nucl. Phys. A 698, 539 (2002); D Adamova *et al.* CERES Collaboration, Phys. Lett. B 666, 425 (2008); G. Agakichiev *et al.*, CERES Collaboration, Eur. Phys. J. C 41, 475 (2005); R. Arnaldi *et al.*, NA60 Collaboration, Eur. Phys. J. C 61, 711 (2009)

[9] A. Ayala *et al.*, Phys. Rev. D 84, 056004 (2011)

[10] P. Colangelo and A. Khodjamirian, in *At the frontier of particle physics/ handbook of QCD*, ed. M. Shifman, World Scientific, Singapore, (2001).

[11] E. Megias, E.R. Arriola, and L.L. Salcedo, Phys. Rev. D 81, 096009 (2010)

[12] C.A. Dominguez and K. Schilcher, JHEP 0701, 093 (2007).

[13] H. Pietschmann, *Formulae and Results in Weak Interactions* (Springer-Verlag 1974).

[14] L.J. Reinders, H. Rubinstein and S. Yazaki, Nucl. Phys. B 186, 109 (1981).

[15] G. Boyd and D.E. Miller, arXiv:hep-ph/9608482 (unpublished), D.E. Miller, arXiv:hep-ph/0008031 (unpublished).

[16] S.H. Lee and K. Morita, J.Phys. G 35, 104024 (2008); S.H. Lee and K. Morita, Phys. Rev. Lett. 100, 022301 (2008)

[17] R.A. Bertlmann *et al.*, Z. Phys. C Particles & Fields 39, 231 (1988); C.A. Dominguez and J. Sola, Z. Phys. C Particles & Fields 40, 63 (1988); C.A. Dominguez and K. Schilcher, JHEP 01, 093 (2007).

[18] V.L. Eletsky, Phys. Lett. B 352, 440 (1995).

[19] L.J. Reinders, H. Rubinstein and S. Yazaki, Phys. Rep. C 127, 1 (1985).

[20] Particle Data Group, C. Amsler *et al.*, Phys. Lett. B 667, 1 (2008).

[21] L. Dolan and R. Jackiw, Phys. Rev. D 268 09, 3320 (1974).

[22] For recent results see e.g. H. Ohno, T. Umeda, and K. Kanaya, J. Phys. G **36**, 064027 (2009), and references therein.

[23] C.A. Dominguez, M. Loewe, J.C. Rojas and Y. Zhang, Phy. Rev. D 83, 034033 (2011).

[24] J. Bordes *et al.*, JHEP 1005 (2010) 064

[25] C.A. Dominguez, M.S. Fetea and M. Loewe, Phys. Lett. B 387, 151 (1996).

[26] Si-xue Qin *et al.*, Phys. Rev. Lett. 106, 172301 (2011).

[27] A. Bazavov *et al.*, Phys. Rev. D 80, 014504 (2009).

[28] S. Schael *et al.*, ALEPH Collaboration, Phys. Rept. 421.

[29] M. Cheng *et al.*, Phys. Rev. D 77, 014511 (2008).

[30] C.A. Dominguez, M. Loewe and Y. Zhang, Phys. Rev. D 86, 034030 (2012)

[31] A. Ayala, C.A. Dominguez, M. Loewe, Y. Zhang, Phys. Rev. D 86, 114036 (2012)